

1 **Knickpoints and Fixpoints: The Evolution of Fluvial Morphology** 2 **under the Combined Effect of Fault Uplift and Dam Obstruction on a** 3 **Soft Bedrock River**

4 Hung-En Chen¹, Yen-Yu Chiu¹, Chih-Yuan Cheng¹ and Su-Chin Chen^{1,2}

5 ¹ Department of Soil and Water Conservation, National Chung Hsing University, Taichung 40227, Taiwan

6 ² Innovation and Development Center of Sustainable Agriculture, National Chung Hsing University, Taichung 40227, Taiwan

7 *Correspondence to:* Su-Chin Chen (scchen@nchu.edu.tw)

8 **Abstract.** Rapid changes in river geomorphology can occur after being disturbed by external factors like earthquakes or large
9 dam obstructions. Studies documenting the evolution of river morphology under such conditions have advanced our
10 understanding of fluvial geomorphology. The Dajia River in Taiwan presents a unique example of the combined effects of a
11 coseismic fault (the 1999 Mw 7.6 Chi-Chi earthquake) and a dam. As a result of the steep terrain and abundant precipitation,
12 rivers in Taiwan have exhibited characteristic post-disturbance evolution over 20 years. This study also considers two other
13 comparative rivers with similar congenital conditions: the Daan River was affected by a thrust fault Chi-Chi earthquake, too;
14 the Zhuoshui River was influenced by dam construction finished in 2001. The survey data and knickpoint migration model
15 were used to analyze the evolution of the three rivers and propose hypothesis models. Results showed that the mobile
16 knickpoint migrated upstream under the influence of flow, while the dam acted as a fixpoint, leading to an increased elevation
17 gap and downstream channel incision. Thereby, the Dajia ~~river~~River narrowing and incision began at both ends and
18 progressively spread to the whole reach under the combined effects.

19 **KEYWORDS:** dam obstruction; fixpoint; coseismic uplift; knickpoint; soft bedrock incision; river evolution

20 1. Introduction

21 Natural tectonic movements and artificial structures are the main factors that disturb river equilibrium. These external
22 influences often interact complexly; therefore, distinguishing between anthropogenic and natural drivers of landscape
23 evolution is difficult. In addition, changes in these external conditions, in turn drive adjustments in the riverbed, generating
24 new landscape patterns. River morphological development generally reflects the geology and flow stress conditions (Lyell,
25 1830). When a significant external impact occurs, a knickpoint (a localized discontinuity in the longitudinal profile of the
26 riverbed) often forms (Holland, 1976). Knickpoints can range in scale from a single waterfall to a zone of several kilometers
27 (Crosby and Whipple, 2006) and may result from natural factors such as extreme weather, sea-level fall, and earthquake-
28 induced surface rupture (Seidl and Dietrich, 1992; Whipple, 2004, Bishop et al., 2005; Heijnen et al., 2020).

29 The active fault causes a prominent knickpoint in stream, known as tectonic uplift, leading to a local increase in channel
30 steepness (Hayakawa et al., 2009; Huang et al., 2013; Cook et al., 2013). The sudden elevation change in the riverbed divides
31 the river profile into two reaches with differing slopes, altering the base level of fluvial erosion. The increasing flow stress
32 erodes the knickpoints, causing it to migrate upstream-ward over time. A long duration is required for the fluvial response to
33 adapt to localized surface uplift or depositional blockage by knickpoint retreat and migration upstream with time, cutting a
34 narrow channel and even forming a canyon. The migration process and speed are highly variable and depend on the tectonic
35 setting and physical nature of the riverbed (Whipple et al., 2004). The emergence and migration of knickpoints caused by
36 disturbance from external conditions was studied extensively (Whipple, 2001; Whipple and Trucker, 2002; Crosby and
37 Whipple, 2006; Clark, 2014; Ahmed et al., 2018).

38 Anthropogenic factors, such as reservoir construction, which is one of the most common ways humans interfere with river
39 hydrology and sedimentation (Magilligan and Nislow, 2005; Petts and Gurnell, 2005; Graf, 2006; Nelson et al., 2013; Liro,
40 2017, 2019; Zhou et al., 2018). Dam as a fixpoint in the river influences two critical components of river geomorphology: the
41 sediment transport capacity of the flow and the oncoming sediment load (Williams and Wolman, 1984). If the sediment
42 transport capacity exceeds the oncoming sediment load, the amount of sediment may be insufficient to maintain the riverbed
43 level, and erosion may occur. Conversely, if the sediment load exceeds the sediment transport capacity, deposition on the
44 riverbed would be expected to occur. The self-adjustment mechanisms of river channels responding to insufficient or excess
45 sediment (Brandt, 2000) results in the change in cross-section geometry, bed material size, river pattern (Leopold and Wolman
46 1957), and slope. Previous studies on the evolution of areas downstream of dams have primarily analyzed changes in

47 downstream sandbars over large spatial scales (Horn et al., 2012; Słowik et al., 2018; Kong et al., 2020) or the ecology of the
48 lower reaches in front of dams (Kingsford, 2000; Braatne et al., 2008; Shafroth et al., 2016). ~~Few~~~~There have been few~~ studies
49 of exposed bedrock have been based on long-term observations (Inbar, 1990). In most cases, a dam effectively traps the
50 sediment supply from the watershed. If sediment transfer to the downstream reaches of the dam is reduced, the armor layers
51 of the riverbed are lost, which may cause an incision of the fluvial channel (Surian and Rindai, 2003). This incision
52 subsequently narrows the river cross-sections and lowers the thalweg level.

53 Decades or hundreds of years are generally required for a riverbed to reach a new equilibrium after disturbance by external
54 conditions, so it is difficult to understand such changes based on short-period observational data (Howard et al., 1994; Tomkin
55 et al., 2003). Because of the abundant rainfall brought by typhoons and monsoons, the river terrain in Taiwan can alter
56 dramatically over a short period of time. Moreover, dams in Taiwan are built primarily in steep reaches, enhancing the rapid,
57 remarkable morphological evolution of the downstream reaches. The reservoirs of dams constructed on the rivers become
58 silted up, resulting in a lack of sediment downstream in the meantime, which causes loss of armor layers, exposure of soft rock,
59 and severe erosion. Another factor influencing the distinctive characteristics of Taiwanese rivers is the geological location;
60 Taiwan is located in a plate junction zone that experiences frequent earthquakes such as the Chi-Chi Earthquake of 1999 (Lin
61 et al., 2001; Ota et al., 2005), which caused the offset of Chelungpu thrust fault in central Taiwan. The surface rupture and
62 uplift induced the formation of knickpoints and river gorges. Twenty years later, the undercutting trend of the active channel
63 below dams and the migration of post-earthquake knickpoints have caused the rivers to evolve into their present forms. This
64 rapid evolution of river morphology over a short time makes Taiwan rivers suitable as case studies. The Dajia River is a unique
65 example, as a dam structure and coseismic uplift impact it simultaneously in a short reach. The current work aims to clarify
66 the river changes caused by the earthquake and a dam, and to propose a hypothesis for the evolution model. To compare the
67 various morphological developments under different external conditions, the Daan, Zhuoshui, and Dajia rivers in central
68 Taiwan are considered in this study.

69 **2. Study area, materials, and methods**

70 The longitudinal changes of the river bed and the accompanying river pattern changes are the objects of observation. A
71 common type of longitudinal profile development for knickpoint retreat is illustrated in Fig. 1a (Gardner 1983; Whipple and
72 Trucker, 1999; Parker and Izumi 2000; Alonso et al. 2002; Bressan et al., 2014). As the base level of erosion fell, the stream
73 encountered an abrupt shift in slope from gentle to steep, which significantly accelerated~~and the abrupt slope caused~~

74 ~~acceleration of the flow, and subsequently led to stream bed erosion of the stream bed. the stream eroded the bed.~~
75 During this process, apparent upstream degradation and downstream aggradation occurred. The knickpoint migrated upward
76 with time, accompanying by slope replacement. After the river had reached a new equilibrium in a channelized pattern, the slope
77 replacement resulted in a natural profile. During the adjustment, the incision trend gradually slowed, and sedimentation may
78 commence downstream (dashed line in Fig. 1a). The profile evolved from a concave curve to a graded profile (Chamberlin
79 and Salisbury, 1904). The well-known result of dam construction is the progressive loss of the armor layer in the neighboring
80 downstream river (Fig. 1b). The scouring baseline extended downstream-ward from the dam (Olsen, 1999; Choi et al., 2005;
81 Słowik et al., 2018). Because of the fixpoint, the local slope at the dam toe became steeper progressively, and the dam caused
82 the downstream river profile to be gentle and sediment transport to decrease.

83 However, significant changes in the longitudinal profile must also be accompanied by variations in river patterns, which
84 have yet to receive much attention. Furthermore, the interaction between fault scarps and dam obstructions within a river reach
85 is rarely observed and studied. To address these gaps, we collected historical data (incl. multiyear satellite images, orthographic
86 images, cross-sectional and longitudinal profiles.) for three rivers in Taiwan (Daan, Zhuoshui, and Dajia), each representing
87 the individual effects of faults and dams, as well as their combined effects.

88 2.1 Study area

89 Taiwan's climate is strongly affected by the western Pacific tropical cyclone. There are approximately three to four
90 typhoons and heavy rain events yearly, and the average annual precipitation is about 2500 mm. The heavy rains during the
91 monsoons and typhoons cause dramatic changes to riverbeds over short periods of time. In addition, because Taiwan is located
92 at the compressive tectonic boundary between the Eurasian and Philippine Sea plates, the collision of the two continental plates
93 causes tectonic breakage of the strata. On September 21, 1999, the Chi-Chi earthquake ($M_w = 7.6$) resulted in uneven uplift in
94 the island. Three central Taiwan rivers illustrate dams or faults' effects (Figure 2): The Daan River has been affected by vertical
95 fault scarps, the Dajia River by both fault scarps and a dam, and the Zhuoshui River by dam obstruction. These three important
96 rivers have very similar characteristics: their east-to-west flow direction; their range of elevation from sea level to ~3000 m;
97 their steep river slopes (the average slope of each river 1.5% – 2.4%, Kuo et al.(2021)the average slopes of the middle and
98 upper reaches are greater than 1/60); and the presence of soft rock in the mid-stream (as shown in the pink region in Figure
99 Fig. 2). The locations of the three rivers and the Chelungpu thrust fault are marked in Figure-Fig. 2. The southern termination
100 of the fault crosses the Zhoushui River trending north-southnorth-south; the northern termination near the Dajia and the Daan

101 rivers shows a complex deformation pattern trending NE–SW to E–W (Lee et al., 2002), composed of several parallel thrust
102 faults. In the three studied reaches, the Pleistocene sedimentary rocks are mainly composed of soft rocks consisting of
103 sandstone, siltstone, shale, and mudstone. Soft rocks have intermediate strength between soils and hard rocks with possessing
104 unconfined compressive strengths ranging from 0.5 to 25.0 MPa (Lai et al., 2011). These rocks are generally poorly lithified
105 and weakened by a high water content; therefore, their resistance to water erosion is poor. The riverbed rock is readily incised
106 by flooding flow when the upper armoring protective layer was lost (Huang et al., 2014).

107 The Chi-Chi earthquake produced a surface rupture 80 km long (Lee et al., 2002). Several fracture planes at the north
108 end of the fault caused uneven uplift in the region (Lee et al., 2002). One of the ruptures passed through the right bank of the
109 Shigang Dam (constructed in 1977) on the Dajia River, causing serious damage to the dam structure. The maximum vertical
110 displacement of the surface rupture was 9 m, increasing the drop height of the bed level between the face and the back of the
111 dam markedly. The dam reconstruction was finished in 2000. The repaired Shigang Dam was intended to store 2.4×10^6 m³
112 of water after the Chi-Chi earthquake; however, owing to deposition in the reservoir, only $\sim 1.4 \times 10^6$ m³ of water can now be
113 retained. After the earthquake and the reconstruction, the fluvial morphology has been changed rapidly. The original armor
114 layers on the riverbed in front of the Shigang Dam were lost rapidly, and the soft bedrock was exposed. The two rupture
115 surfaces at the north end of the Chelungpu Fault uplifted a 1 km reach of bed in the Daan River, with a maximum vertical
116 uplift of 10 m.

117 Although the southern end of the Chelungpu Fault passes downstream of the Jiji Dam (Zhuoshui River), the fault uplifted
118 the bed level by ~ 2 m, less than the uplifts in the Daan and Dajia rivers. The Jiji Dam was built in 2001 (after the 1999 Chi-
119 Chi earthquake), is situated on the narrowest part of the Zhuoshui River, and has a maximum designed storage capacity of 10
120 $\times 10^6$ m³. Due to the large sediment yield in the Zhuoshui River watershed, the present-day adequate water storage capacity is
121 only $\sim 4 \times 10^6$ m³. The Jiji Dam downstream is known for its soft bedrock canyon features, formed by dam-obstructed water
122 scouring.

123 2.2 Materials

124 Analysis of the effects of faults and dams, alteration of river patterns, changes in thalweg levels, and variations in river
125 cross-sections are crucial to revealing the process of river evolution. SPOT-5 and SPOT-6 satellite images (2 m in
126 resolutions) and orthographic images (25 – 50 m in resolutions) obtained by the Center for Space and Remote Sensing
127 Research, National Central University (CSRSR/NCU) and the Aerial Survey Office (AFASI) of Taiwan were used to

128 assess changes in river patterns. Multiyear cross-sectional and longitudinal profiles were established from historical
 129 surveys by the Water Resources Agency (WRA). The survey was conducted using Total Station, GPS, and depth sounder.
 130 The interval of survey points should be 5–10 m, and the elevation error must not exceed cm. Additional analyses of
 131 knickpoint retreat and variations in river elevation and width were carried out. The locations of knickpoints were
 132 determined by identifying abrupt terrain changes and the positions of splash in the images. In order to analyze the
 133 variation of channel width (W), depth (D), and aspect ratio (W/D), we calculated the bank-full discharge width and depth,
 134 which represents the maximum flow that can occur in a river before water starts overflowing and spreading out onto the
 135 floodplain. We identified the river banks and extracted channel widths from orthographic images. The banks were defined
 136 as the boundaries between the main channel and the adjacent floodplain.

137 2.3 Mathematical model

138 The application of the mathematical model provides an abstract description of a concrete system using physical concepts
 139 and mathematical language. A one-dimensional Exner equation (Exner, 1925) is used to describe the advective and diffusive
 140 knickpoint migration (Bressan et al., 2014):

$$141 \quad \frac{\partial z}{\partial t} + \frac{1}{(1-p_s)} \frac{\partial q_s}{\partial x} = 0 \quad (1a)$$

142 where z is the bed elevation along the thalweg, p_s is the porosity of bed sediment, t is the time, x is the distance, and q_s is
 143 the sediment discharge per unit width that is estimated by the product of the surface height change η , and the knickpoint
 144 migration rate dx/dt is expressed as equation 1b.

$$145 \quad q_s = -\eta \frac{dx}{dt} \quad (1b)$$

146 The migration rate as a sediment separation per unit area homogeneously distributed over the eroding surface is expressed
 147 as equation (1c).

$$148 \quad \frac{dx}{dt} = k_d [\tau(x) - \tau_c] \quad (1c)$$

149 where k_d is the erodibility, τ is the bed shear stress, and τ_c is the critical shear stress of the bed material. The condition of
 150 an obvious knickpoint face, τ should be estimated using a formula that considers knickpoint as a submerged obstacle
 151 (equation (1d)) (Engelund, 1970).

$$152 \quad \tau(x) = M\tau_0 \left[1 + A \frac{(z-z_0)}{H_0} + B \frac{\partial z}{\partial x} \right] \quad (1d)$$

153 The factors M , A , and B in equation (1d) are parameters related to localized phenomena. τ_0 , z_0 , and H_0 are the shear
 154 stress, bed elevation and the water depth upstream of the knickpoint. The term $B \frac{\partial z}{\partial x}$ represents the change in shear stress due

155 to the local slope. The shear stress in the channel section upstream of the knickpoint crest ($\tau_0 = \gamma H_0 S_0$, where γ is the specific
156 weight of water changes across the knickpoint due to the abrupt change in bed topography (equation (1d)). Substituting
157 equations (1b)–(1d) into equation (1a), equations (2a)–(2c) were obtained in below:

$$158 \quad \frac{\partial z}{\partial t} - C \frac{\partial z}{\partial x} - D \frac{\partial^2 z}{\partial x^2} = 0 \quad (2a)$$

$$159 \quad C = \left(\frac{\eta^k d \gamma}{1 - p_s} \right) S_0 M A \quad (2b)$$

$$160 \quad D = \left(\frac{\eta^k d \gamma}{1 - p_s} \right) S_0 H_0 M B \quad (2c)$$

161 where the coefficients of the first- and second-order spatial derivatives, C and D , are known as the advection and diffusion
162 coefficients, respectively. It can be concluded that the key controls of the knickpoint retreat are the channel slope, the erodibility
163 of the bed of the river reach, the knickpoint face height, and the upstream water depth. Therefore, the present equation is a
164 physical-based model that can be solved with the second-order accurate implicit finite difference scheme which was
165 implemented in MATLAB. [However, it is essential to recognize that the numerical model is conceptual and involves several](#)
166 [assumptions, such as not considering variations in the horizontal 2D plane of the terrain and assuming homogeneous](#)
167 [parameters within the simulation area, among others. The numerical model cannot fully capture the actual scenario's detailed](#)
168 [morphology and environmental conditions; it serves as a conceptual model based on physical mechanisms, providing trends](#)
169 [rather than precise representations.](#)

170 3. RESULTS

171 3.1 Fault effect on Daan River canyon

172 The scarps across the Daan River that were uplifted by the Chi-Chi earthquake caused a dramatic change in the topography,
173 disturbing the dynamic equilibrium of the fluvial system. Cook et al. (2013) proposed that the knickpoint propagated rapidly
174 after 2004 and pointed out that, ~~after the disappearance of bedload~~, the tool effect caused pronounced fluvial incision of the
175 bedrock ~~after the disappearance of bedload~~. Knickpoint propagation was influenced by the antiformal geological structure of
176 the area, the presence and orientation of interbedded strong and weak lithologies, and the proportion of discharge entering the
177 main channel. Huang et al. (2013) also proposed that the knickpoint retreat rate can be affected by several factors, including
178 discharge, rock properties, geological structures, and bedrock orientation. The channel development of the studied reach and
179 the behavior of knickpoint retreat were assessed by analyzing multiyear data on the form and cross-section of the river.

180 Successive orthographic images of the studied reach of the Daan River from 2000 to 2017 and the corresponding flow

181 paths are illustrated in Fig. 3. River cross-sections constructed from precise survey data are provided in Fig. 4. Chronological
182 longitudinal profiles of the river reach are shown in Fig. 5. Longitudinal profile data from Cook et al. (2013) were included to
183 make information more complete. The effect of the earthquake on the surface elevation is clearly visible in Fig. 5. In addition
184 to the survey data, the advective and diffusive knickpoint migration model (equation 2) was solved to mathematize the
185 knickpoint retreat progress after the Chi-Chi earthquake. The initial condition and boundaries condition are needed to solve
186 the equation. The initial condition is the longitudinal profile in 1999, while the boundary conditions are the real bed changes
187 in upstream and downstream boundaries. The C and D are physical parameters and were calibrated by the survey data. In
188 equation 2, C represents the moving speed, and D represents the diffusion constant. These two coefficients reflect the rate of
189 bed erosion, which is physically composed mainly of bed shear stress (equations 2b and 2c). Due to the actual bed erosion
190 rates varying with time, the parameters were adjusted to match the real changes. Before 2004, C was 22.0 m/yr, and D was
191 $10.0 \text{ m}^2/\text{yr}$; after 2004, C was 91.5 m/yr, and D was $18.5 \text{ m}^2/\text{yr}$, and the simulation was continued until 2011 when the
192 knickpoint disappear. The result of the modeling is shown at the top left corner in Fig. 5. The knickpoint progressively retreats,
193 accompanying by slope replacement. The variation trend of the simulation and survey data is generally consistent, and the speed
194 (C) has a larger value in 2004_–_2011, which is also consistent with the observation.

195 The long-term development of the studied reach of the Daan River in the past 20 years, after the coseismic uplift, can be
196 divided into three periods: downstream erosion and slow knickpoint migration (earthquake to 2004); sudden migration of the
197 knickpoint (2004_–_2011); and gorge widening and eradication (2011_–_present).

198 **3.1.1 Downstream erosion and slow knickpoint migration (earthquake to 2004)**

199 After the Chi-Chi earthquake, coseismic ground deformation created a pop-up obstruction across the river, forming a
200 barrier lake behind the rupture scarp. The obstacle blocked the river flow and trapped the sediment, causing the river bed
201 downstream of the rupture scarp completely lose the armor layer. When the armor layer was lost, bedrock incision occurred
202 downstream of the uplifted zone, and the knickpoint retreat appeared. On the other hand, no significant erosion occurred
203 between cross-sections **a** and **b** during that period (Figs 3 and 4). A comparison of the cross-sections for 2000 and 2004 (Fig.
204 4) reveals that most parts of the section **a** even experienced deposition. Slight erosion in some places can be detected in the
205 longitudinal profiles (Fig. 5) between 1999 (after the earthquake) and 2004. Although the seismic uplift produced an obvious
206 knickpoint on the riverbed, that knickpoint migrated only slightly (85 m; Table 1) between 2000 and 2004. The downstream
207 reach of the uplifted zone showed evidence of scour, but no noticeable bedrock incision or canyon landscape had developed

208 yet.

209 3.1.2 Sudden migration of knickpoint (2004–2011)

210 The orthographic image for 2007 (Fig. 3) clearly shows that the armor layer had been removed, the bedrock had been
211 exposed, and the deep incision had formed a narrow channel. The knickpoint retreated upstream-ward by approximately 422
212 m between 2004 and 2007, accompanied by continued scouring downstream. In the uplifted reach, under the stress of the
213 concentrated flow in the newly formed channel, the tool effect resulted in a deepened incision of the rock bed, and a canyon
214 landform gradually developed. In the 2007 cross-section data for section **a**, a canyon close to the left bank can be observed,
215 which persisted until 2011. A rapid incision rate (5.6 m/yr) occurred in section **a**, which also experienced a narrowing rate of
216 about 105.5 m/yr. Bed incision and narrowing of the main channel occurred in section **b** simultaneously, with a narrowing rate
217 of approximately 89.9 m/yr and an incision rate of about 2.1 m/yr. Between 2007 and 2011, the knickpoint retreated upstream
218 by about 412 m; the incision at section **a** was lessened, but section **b** experienced a notable incision into the rock bed
219 accompanied by knickpoint retreat. Because an obvious gorge channel had appeared in the uplifted zone, sediment from
220 upstream was transported downstream, and downstream scouring transformed gradually into sedimentation; therefore, the
221 convex longitudinal profile was gradually erased.

222 3.1.3 Gorge widening and eradication (2011 to the present)

223 After 2011, the knickpoint became insignificant in the longitudinal profile, so the thalweg scouring trend slowed. The
224 morphology development is dominated by lateral erosion instead of vertical incision. The narrow, deep canyon evolved into a
225 U-shaped canyon with a wide bottom. River pattern migration from upstream caused the canyon-type channel to commence
226 transforming into a braided channel. The main channel of section **a** experienced deposition as a result of the sediment supply
227 being adequate (Fig. 5). Cook et al. (2014) proposed a mechanism of gorge eradication, called *downstream sweep erosion*,
228 which rapidly transformed the gorge into a beveled floodplain through the downstream propagation of a wide erosion front
229 located where the broad upstream channel abruptly became a narrow gorge. The sweep boundary is clearly visible in the
230 orthographic images for 2011 and 2017 (Fig. 3). Additional large floods are expected to cause a marked widening of the channel
231 instead of deepening (Huang et al., 2013). It has been estimated that removal of the gorge erosion will take 50 years (Cook et
232 al., 2014).

233 Significant incision of the channel is common after a riverbed has been uplifted suddenly by ~~topographic~~-tectonic
234 movement and the bed slope changes dramatically (Merritts et al., 1989). This was the case for the Daan River after the Chi-

235 Chi earthquake. After the coseismic uplift, the base level of erosion downstream reduced, so erosion increased. The river width
236 became notably narrower and deeper. Upward movement of the knickpoint caused the river channel in the uplifted section to
237 narrow rapidly. The concentrated flow caused a rapid incision of a weak geological layer in the riverbed, so the channel width
238 decreased sharply. Therefore, the uplifted section formed a canyon landform. As the slope at the knickpoint gradually recovered,
239 the incision slowed and sediment transport down the recovered river resulted in sediment deposition in the downstream channel.
240 The river also gradually developed lateral erosion upstream, and the river channel tended to widen. The channelization is
241 expected to have been swept because the sweep boundary migrated progressively downward.

242 3.2 Jiji Dam effect on Zhoushui River

243 Construction of the Jiji Dam on the Zhoushui River began in 1996 and operated in 2001. Orthographic images, flow paths
244 of the studied reach, and the locations of cross-sections **c**, **d**, and **e** below the Jiji Dam for 1998 to 2018 are provided in Fig. 6.
245 Chronological survey data of cross-sections **c**, **d**, and **e** are provided in Fig. 7. Chronological longitudinal profiles of the studied
246 reach are illustrated in Fig. 8. The river is located at the southern termination of the Chelungpu Fault (Fig. 1), where the
247 elevation gap caused by the earthquake is relatively small. In 1998, the Zhoushui River was a broad braided river, with many
248 sandbars downstream of the dam (Fig. 6). In 2003, two years after dam operation had commenced, the riverbed armor layer
249 had been lost and the exposed soft bedrock was clearly visible within 700 m of the toe of the dam, because of a lack of sediment.
250 The bedrock's incision deepened due to the tool effect, and the flow path concentrated gradually in front of the dam. From
251 2003 to 2007, the effect zone gradually expanded, and exposed bedrock extended to ~3.2 km downstream from the dam. ~~The~~
252 ~~bedrock's incision deepened due to the tool effect, and the flow path concentrated gradually in front of the dam.~~ Between 2007
253 and 2018, the channelization and the zone with exposed bedrock expanded continuously to 6.5 km downstream of the dam.
254 Due to the channelization, the river cross-section became narrow and deep.

255 The transformation of the river and the rates of lateral and vertical change are clearly visible in the river cross-sections
256 (Fig. 7). There was no apparent erosion of section **c** in 2008, but the sections closer to the dam (**d** and **e**) exhibited obvious
257 incision (Fig. 7). After the loss of the riverbed armor layer, the flow cut down into weak bedrock. The deep main channels'
258 development is clearly visible in sections **d** and **e** between 1998 and 2008. During this time, the incision rate of section **e** was
259 around 1.2 m/yr, and the narrowing rate was around 25 m/yr. During 2008–2012, engineering measures were installed:
260 Between section **d** and section **e**, groundsills, spur dikes and tetrapod were added to the river channel to prevent erosion, and
261 the riverbed level rose slightly at section **e**. However, the channel width of section **c** was markedly narrower, with a narrowing

262 rate of roughly 65 m/yr. Between 2008 and 2015, the incision rates of sections **c** and **d** were roughly 1.4 m/yr. ~~Stratified~~
263 ~~Progressive~~ erosion layer by layer is apparent in the chronological longitudinal profiles (Fig. 8). Incision of the studied reach
264 became increasingly severe: incision commenced at section **e** and subsequently extended downstream to sections **d** and **c**. We
265 infer that headward erosion did not dominate the riverbed because the Chelungpu Fault passed through the river some distance
266 from the dam and caused only 2 m of uplift; on the contrary, dam-induced downward incision of the riverbed caused
267 degradation of the reach. There is an approximately 15 m difference between the bed level of 1998 and that of 2018.

~~The studied reach of the Zhoushui River was a braided river prior to building of the dam. After dam construction, sediment
268 transport was restricted, causing loss of the armor layer downstream under the influence of the tool effect, a deeply incised
269 channel formed in the weak soft bedrock in front of the dam. The flow gradually became concentrated in the deep channel, the
270 river width decreased markedly, and the effect continued to extend downstream with time.~~

272 3.3 The combined effect of Shigang Dam and Fault on Dajia River

273 The studied reach of the Dajia River, which lies downstream of the Shigang Dam, was affected by both the dam and uplift
274 caused by the Chi-Chi earthquake. The Shigang Dam was broken by uneven uplift of the fault scarp across the dam (9 m on
275 the right side and 3 m on the left), and the downstream section **f** rose by ~7 m (see Fig. 2). The earliest knickpoint formed close
276 to section **f**: ~~and moving~~ The base level of erosion declined downstream after uplift causing the knickpoint to move headward
277 with time. During 2000–2005, the knickpoint retreated by ~~~40400~~ m, and another new knickpoint formed between sections **g**
278 and **h** (Fig. 9) under the co-effect of river pattern changes and bed rock differential erosion.—The damming effect of the
279 Shigang Dam also caused the armor layer to be removed. The bedrock became exposed shortly after the earthquake; however,
280 section **f** was obviously incised during 2000–2005, whereas incision of section **g** did not occur until 2005–2008 (Fig. 10).
281 Between 2000 and 2005, engineering measures were installed on several occasions to mitigate the obvious erosion. The river
282 pattern between section **g** and the dam ~~was~~ were ~~a braided river during the period. Groundsills and energy dissipation measures~~
283 ~~were constructed in front of the dam; as a result, the flow path between section **g** and the dam became a floodplain.~~

284 The incision rate of section **g** was ~1.1 m/yr during 2005–2008, and the narrowing rate was ~47.7 m/yr. During the same
285 time interval, the downstream knickpoint (between sections **f** and **g**) disappeared due to river training in 2008. The knickpoint
286 between section **g** and section **h** retreated rapidly toward the dam (Figs 9, 11). During 2005–2008 and 2008–2017, the
287 knickpoint moved upstream by approximately 186 and 219 m, respectively. This retreat of the knickpoint implies that river
288 channel scouring did not stop. Because the riverbed strata trend northeast–southwest, flow scouring preferentially deepened

289 the left part of the rock bed, which moved the channel closer to the left bank. After 2008, the flow channel extended closer to
290 the toe of the dam. Due to the severe incision, the government started surveying section **h** after 2010 (Fig. 10). Significant
291 bedrock incision was recorded, with an incision rate of ~ 1.4 m/yr at section **h** during 2010–2017. In 2008, it can be observed
292 that the knickpoint existed in the reach between sections **g** and **h**; therefore the slope of the channel is still discontinuous. ~~The~~
293 ~~channel starting from the toe of the dam was not connected with the channel caused by headward erosion from section **f** (Fig.~~
294 ~~9) until 2017.~~ The 2017 photograph shows a single, meandering channel that starts from the dam and runs through sections **h**
295 and **g**, eventually reaching section **f**, where the knickpoint had initially formed (Fig. 10). Overall, the area downstream of the
296 Shigang Dam displayed headward erosion of the knickpoint and incision of the rock bed in front of the dam.

297 In the Dajia River, the advection and diffusion equation (equation 2) was also used to represent the variation mode of
298 knickpoint and bed elevation. The initial condition is the longitudinal profile in 2000. The coefficients C and D were influenced
299 by bed shear stress. Due to the rapid increase in actual bed erosion rate after 2005, the parameters were adjusted to match the
300 actual changes. Before 2005, C was 7.5 m/yr, and D was 1.825 m²/yr; after 2005, C was 36.5 m/yr, and D was 9.125 m²/yr, and
301 the simulation was continued until 2017. The downstream boundary adopts the real bed change, while the upstream boundary
302 condition is fixed, considering the dam is a fixed point. The bed is progressively scoured in the nearby downstream of the dam,
303 and the knickpoint retreats and gradually fades away. The variation trend of the simulation and survey is generally consistent,
304 excluding the fact that intensive engineering works have been conducted in front of the dam to stabilize the bed.

305 4. Discussion

306 Data on the changes in the riverbed, river width, and migration distance of the knickpoint for all three studied reaches are
307 provided in Table 1. Also, in Fig. 12(a), We use “**T**” symbols to represent the channel width (W) and depth (D) of the cross-
308 sections in three study reaches. ~~The, and the~~ aspect ratio (W/D) is labeled above every “**T**.” After the Chi-Chi earthquake, the
309 channel geometry was not disturbed immediately. ~~The, and the~~ aspect ratio of the Daan River exhibited only slight changes.
310 Consequently, the aspect ratio ~~thatweg~~ significantly decreased with time from the downstream section; subsequently, the aspect
311 ratio ~~thatweg~~ recovered a little after 2011. The deepening of the upstream was slower than that downstream, but the later
312 recovery was more obvious in the upstream area. The aspect ratio of the Zhuoshui River dramatically declined in the upstream
313 part after construction of the Jiji Dam; this change extended gradually to the downstream section with time. In the Dajia River,
314 owing to the combined effects of the upstream dam and the earthquake, channelization of the river started at both ends of the
315 reach and then met in the middle. The examples of these three rivers allow us to deduce the evolution of knickpoint retreat and

316 transformation of the river pattern under the influence of dams and/or uplift.

317 The river pattern of knickpoint retreat is illustrated in Fig. 12(b), and it was also observed in the Daan River. During the
318 knickpoint retreat, the tool effect caused the river to narrow dramatically. However, after the river had reached a new
319 equilibrium in a channelized pattern, the slope replacement resulted in a natural profile. The incision trend gradually slowed
320 during the adjustment, and sedimentation may commence downstream (dashed line in Fig. 12(b)). The profile evolved from a
321 concave curve to a graded profile (Chamberlin and Salisbury, 1904). In the case of the Daan River, the topography of the
322 upstream gorge was gradually swept away, and the river pattern may be slowly restored to the original braided plain.

323 Before construction of the Jiji Dam, the studied reach of the Zhoushui River was a broad braided river. The river armor
324 layer was lost due to sediment trapping by the dam. Under the influence of the tool effect, the flow path in front of the dam
325 gradually narrowed (Fig. 12(c)). The scouring boundary extended downstream-ward from the dam. Because of the immovable
326 knickpoint, the local slope at the dam toe became steeper, and the dam (acting as a non-erasable knickpoint) caused the river
327 profile and sediment transport to remain non-equilibrium-state.

328 The reach downstream of the Shigang Dam on the Dajia River was simultaneously affected by coseismic uplift and the
329 incision of a deep path in the soft rock in front of the dam. The knickpoint caused by fault uplift retreated upward with time.
330 Although the uplift of the Dajia River was similar to that of the Daan River, the Shigang Dam (fixpoint) restricted knickpoint
331 retreatment in the Dajia River, and led to scouring downward from the dam site. Therefore, we saw the river narrowing at the
332 two ends of the affected reach, then progressively extending to the middle, as shown in Fig. 12(d). The knickpoint caused by
333 the earthquake was gradually removed, but the effect of the dam remains. Therefore, the start of recovery to a braided river
334 cannot happen in the Dajia River.~~the restoration of the Daan River cannot be seen in the Dajia River.~~

335 In Fig 13, the discharge data of outflow from Shigang Dam (Dajia River) and Jiji Dam (Zhuoshui River), and the flow
336 data of the Daan River from July 2005 to December 2019. The cumulative flow results show that the increasing trends of the
337 discharge in the Dajia and Zhuoshui Rivers are consistent. Both dams serve the purpose of controlling water levels for water
338 supply and irrigation. The direct discharge is influenced by the variations in dry and rainy seasons, resulting in intermittent
339 changes in the discharge. In contrast, the flow in the Daan River shows continuously and stable increasing. We observed a
340 positive correlation between the knickpoints retreat distances and the cumulative discharge in the Dajia River and also in Daan
341 River. However, the correlation between flow and retreat distance does not exist when comparing different rivers. Additionally,
342 A relationship between discharge and the changes in channel widening or the incision depth cannot be found.

343 Overall, there are apparent differences in the morphological changes to rivers caused by natural and human factors. A
344 knickpoint formed by fault-induced riverbed uplift is a moving point: as the knickpoint moves, the riverbed evolves gradually
345 from an unstable state to an equilibrium. ~~Topographic development is like the process of childhood to old age (Davis, 1899).~~
346 In contrast, a dam can be regarded as a fixpoint on the river. The flow from the spillway outlet hits the riverbed continuously,
347 resulting in a decline of the erosion base level; therefore, downward erosion commences from the toe of the dam. ~~To summarize,~~
348 ~~changes resulting from natural tectonic movements of a riverbed may achieve equilibrium with time, whereas imbalance~~
349 ~~caused by anthropogenic structures may be enhanced with time. Therefore,~~ For the case under the combined effect of fault
350 uplift and dam obstruction, we inferred a schematic diagram of longitudinal profile development for the combined effects as
351 shown in Fig. ~~1314~~. In Fig 134, the uplift creates knickpoints that gradually retreat upstream. Meanwhile, Starting from the
352 dam toe, the continuous deepening. When these two phenomena meet, ~~To summarize,~~ changes resulting from natural tectonic
353 movements of a riverbed may achieve equilibrium with time, whereas imbalance caused by anthropogenic structures may be
354 enhanced with time. ~~Therefore,~~

355 5. Conclusions

356 The Daan River, Zhoushui River, and Dajia River in central Taiwan exhibited changes in river morphology after
357 disturbance by earthquake uplift and dam obstruction during the past 20 years. The Daan River was affected by a thrust fault;
358 the Zhoushui River was influenced by dam obstruction; and the Dajia River was both fault- and dam-influenced. In the Daan
359 River, the greater slope accelerated the flow velocity and drove knickpoint retreat after removal of the armor layer, resulting
360 in the progress of slope replacement. However, the incision faded with time, sediment deposition commenced, and the river
361 showed potential for recovery to braided river pattern. Because of sediment trapping by the Jiji Dam, the Zhoushui River has
362 transformed from braided to gorge. The channelization started from the dam and expanded downward, and the incision progress
363 caused the local slope at the toe to become steeper. Because the dam acts as an immovable knickpoint, the river's sediment
364 equilibrium could not be re-established. The Shigang Dam on the Dajia River also caused a downward incision. The incision
365 from the toe of the dam subsequently connected with the knickpoint retreat caused by headward erosion from downstream,
366 forming a single, meandering channel at the front of the dam.

367 Knickpoints resulting from fault-induced riverbed uplift are moving points: as the knickpoint moves, the riverbed
368 evolves gradually from an unstable state to an equilibrium state. In contrast, a dam, as a fixpoint on the river, causes continuous
369 degradation. When both effects exist on a reach, the impact of the knickpoint gradually fades away, but the results of the dam

370 on the river persist.

371 **Author contribution.**

372 ~~The authors made the following contributions~~The following contributions were made by the authors: HEC was involved
373 in methods development, modeling, data analysis, discussion, and paper preparation. YYC participated in data analysis,
374 discussion, and paper preparation. CYC conducted the field survey, collected and analyzed data. SCC contributed to the
375 hypothesis, concept, research design, conclusions, and paper preparation.

376 **Competing interests.**

377 The authors declare that they have no conflict of interest.

378 **Acknowledgements.**

379 The Ministry of Science and Technology, Taiwan, partially supports this research under grant No. 111-2625-M-005-001.
380 The authors would like to thank AFASI, MOST, and CSRSR/NCU for supplying satellite imagery data; and ~~thank~~ WRA for
381 supplying river measurement data.

382 **References**

- 383 Ahmed, M. F., Rogers, J. D., and Ismail, E. H.: Knickpoints along the upper Indus River, Pakistan: an exploratory survey of
384 geomorphic processes, *Swiss Journal of Geosciences*, 111, 191-204, <https://doi.org/10.1007/s00015-017-0290-3>, 2018.
- 385 Alonso, C. V., Bennett, S. J., and Stein, O. R.: Predicting head cut erosion and migration in concentrated flows typical of
386 upland areas, *Water Resources Research*, 38, 39-31-39-15, <https://doi.org/10.1029/2001wr001173>, 2002.
- 387 Bishop, P., Hoey, T. B., Jansen, J. D., and Artza, I. L.: Knickpoint recession rate and catchment area: the case of uplifted
388 rivers in Eastern Scotland, *Earth Surface Processes and Landforms*, 30, 767-778, <https://doi.org/10.1002/esp.1191>, 2005.
- 389 Braatne, J. H., Rood, S. B., Goater, L. A., and Blair, C. L.: Analyzing the impacts of dams on riparian ecosystems: a review
390 of research strategies and their relevance to the Snake River through Hells Canyon, *Environmental Management*, 41, 267-
391 281, <https://doi.org/10.1007/s00267-007-9048-4>, 2008.
- 392 Brandt, S. A.: Classification of geomorphological effects downstream of dams, *Catena*, 40, 375-401,
393 [https://doi.org/10.1016/S0341-8162\(00\)00093-X](https://doi.org/10.1016/S0341-8162(00)00093-X), 2000.
- 394 Bressan, F., Papanicolaou, A. N., and Abban, B.: A model for knickpoint migration in first- and second-order streams,
395 *Geophysical Research Letters*, 41, 4987-4996, <https://doi.org/10.1002/2014GL060823>, 2014.
- 396 Chamberlin, T. C., and Salisbury, R. D.: *Geology: Geologic processes and their results*, H. Holt, 1904.
- 397 Choi, S. U., Yoon, B., and Woo, H.: Effects of dam-induced flow regime change on downstream river morphology and
398 vegetation cover in the Hwang River, Korea, *River Research and Applications*, 21, 315-325, <https://doi.org/10.1002/tra.849>,
399 2005.
- 400 Clark, M. K., Maheo, G., Saleeby, J., and Farley, K. A.: The non-equilibrium landscape of the southern Sierra Nevada ,
401 California, 5173, [https://doi.org/10.1130/1052-5173\(2005\)15](https://doi.org/10.1130/1052-5173(2005)15), 2014.
- 402 Cook, K. L., Turowski, J. M., and Hovius, N.: A demonstration of the importance of bedload transport for fluvial bedrock
403 erosion and knickpoint propagation, *Earth Surface Processes and Landforms*, 38, 683-695, <https://doi.org/10.1002/esp.3313>,
404 2013.
- 405 Cook, K. L., Turowski, J. M., and Hovius, N.: River gorge eradication by downstream sweep erosion, *Nature Geoscience*, 7,
406 682-686, <https://doi.org/10.1038/ngeo2224>, 2014.
- 407 Crosby, B. T., and Whipple, K. X.: Knickpoint initiation and distribution within fluvial networks: 236 waterfalls in the
408 Waipaoa River, North Island, New Zealand, *Geomorphology*, 82, 16-38, <https://doi.org/10.1016/j.geomorph.2005.08.023>,
409 2006.
- 410 ~~Davis, W. M.: Rivers and valleys of Pennsylvania, *Geographical essays by William Morris Davis*, 413-513, 1889.~~
- 411 ~~Engelund, F.: Instability of erodible beds, *Journal of Fluid Mechanics*, 42, 225-244,~~
- 412 ~~<https://doi.org/10.1017/S0022112070001210>, 1970.~~
- 413 Gardner, T. W.: Experimental study of knickpoint and longitudinal profile evolution in cohesive, homogeneous material,
414 *Geological Society of America Bulletin*, 94, 664-672, 1983.
- 415 Graf, W. L.: Downstream hydrologic and geomorphic effects of large dams on American rivers, *Geomorphology*, 79, 336-
416 360, <https://doi.org/10.1016/j.geomorph.2006.06.022>, 2006.
- 417 Hayakawa, Y. S., Matsuta, N., and Matsukura, Y.: Rapid recession of fault-scarp waterfalls: Six-year changes following the
418 921 Chi-Chi Earthquake in Taiwan, *Chikei/Transactions, Japanese Geomorphological Union*, 30, 1-13, 2009.
- 419 Heijnen, M. S., Clare, M. A., Cartigny, M. J. B., Talling, P. J., Hage, S., Lintern, D. G., Stacey, C., Parsons, D. R., Simmons,
420 S. M., Chen, Y., Sumner, E. J., Dix, J. K., and Hughes Clarke, J. E.: Rapidly-migrating and internally-generated knickpoints
421 can control submarine channel evolution, *Nature Communications*, 11, 3129-3129, [https://doi.org/10.1038/s41467-020-
422 16861-x](https://doi.org/10.1038/s41467-020-16861-x), 2020.

423 Holland, W. N., and Pickup, G.: Flume study of knickpoint development in stratified sediment, *Geological Society of*
424 *America Bulletin*, 87, 76-82, [https://doi.org/10.1130/0016-7606\(1976\)87<76:FSOKDI>2.0.CO;2](https://doi.org/10.1130/0016-7606(1976)87<76:FSOKDI>2.0.CO;2), 1976.

425 Horn, J. D., Joeckel, R. M., and Fielding, C. R.: Progressive abandonment and planform changes of the central Platte River
426 in Nebraska, central USA, over historical timeframes, *Geomorphology*, 139, 372-383,
427 <https://doi.org/10.1016/j.geomorph.2011.11.003>, 2012.

428 Howard, A. D., Dietrich, W. E., and Seidl, M. A.: Modeling fluvial erosion on regional to continental scales, *Journal of*
429 *Geophysical Research*, 99, <https://doi.org/10.1029/94jb00744>, 1994.

430 Huang, M.-W., Pan, Y.-W., and Liao, J.-J.: A case of rapid rock riverbed incision in a coseismic uplift reach and its
431 implications, *Geomorphology*, 184, 98-110, <https://doi.org/10.1016/j.geomorph.2012.11.022>, 2013.

432 Huang, M. W., Liao, J. J., Pan, Y. W., and Cheng, M. H.: Rapid channelization and incision into soft bedrock induced by
433 human activity - Implications from the Bachang River in Taiwan, *Engineering Geology*, 177, 10-24,
434 <https://doi.org/10.1016/j.enggeo.2014.05.002>, 2014.

435 Inbar, M.: EFFECT OF DAMS ON MOUNTAINOUS BEDROCK RIVERS, *Physical Geography*, 11, 305-319,
436 <https://doi.org/10.1080/02723646.1990.10642409>, 1990.

437 Kingsford, R. T.: Ecological impacts of dams, water diversions and river management on floodplain wetlands in Australia,
438 *Austral Ecology*, 25, 109-127, <https://doi.org/10.1046/j.1442-9993.2000.01036.x>, 2000.

439 Kong, D., Latrubesse, E. M., Miao, C., and Zhou, R.: Morphological response of the Lower Yellow River to the operation of
440 Xiaolangdi Dam, China, *Geomorphology*, 350, 106931-106931, <https://doi.org/10.1016/j.geomorph.2019.106931>, 2020.

441 [Kuo, C.-W., Tfwala, S., Chen, S.-C., An, H.-P., and Chu, F.-Y.: Determining transition reaches between torrents and](https://doi.org/10.1002/hyp.14393)
442 [downstream rivers using a valley morphology index in a mountainous landscape, *Hydrological Processes*, 35, e14393,](https://doi.org/10.1002/hyp.14393)
443 <https://doi.org/10.1002/hyp.14393>, 2021.

444 [Lai, Y. G., Greimann, B. P., and Wu, K.: Soft Bedrock Erosion Modeling with a Two-Dimensional Depth-Averaged Model,](https://doi.org/10.1061/(asce)hy.1943-7900.0000363)
445 [Journal of Hydraulic Engineering, 137, 804-814, \[https://doi.org/10.1061/\\(asce\\)hy.1943-7900.0000363\]\(https://doi.org/10.1061/\(asce\)hy.1943-7900.0000363\), 2011.](https://doi.org/10.1061/(asce)hy.1943-7900.0000363)

446 Lee, J. C., Chu, H. T., Angelier, J., Chan, Y. C., Hu, J. C., Lu, C. Y., and Rau, R. J.: Geometry and structure of northern
447 surface ruptures of the 1999 Mw = 7.6 Chi-Chi Taiwan earthquake: Influence from inherited fold belt structures, *Journal of*
448 *Structural Geology*, 24, 173-192, [https://doi.org/10.1016/S0191-8141\(01\)00056-6](https://doi.org/10.1016/S0191-8141(01)00056-6), 2002.

449 [Leopold, L. B. and Wolman, M. G.: River channel patterns: braided, meandering, and straight, US Government Printing](https://www.gpo.gov/docid/1957/)
450 [Office, 1957.](https://www.gpo.gov/docid/1957/)

451 Lin, A., Ouchi, T., Chen, A., and Maruyama, T.: Co-seismic displacements, folding and shortening structures along the
452 Chelungpu surface rupture zone occurred during the 1999 Chi-Chi (Taiwan) earthquake, *Tectonophysics*, 330, 225-244,
453 [https://doi.org/10.1016/S0040-1951\(00\)00230-4](https://doi.org/10.1016/S0040-1951(00)00230-4), 2001.

454 Liro, M.: Dam-induced base-level rise effects on the gravel-bed channel planform, *Catena*, 153, 143-156,
455 <https://doi.org/10.1016/j.catena.2017.02.005>, 2017.

456 Liro, M.: Dam reservoir backwater as a field-scale laboratory of human-induced changes in river biogeomorphology: A
457 review focused on gravel-bed rivers, *Science of the Total Environment*, 651, 2899-2912,
458 <https://doi.org/10.1016/j.scitotenv.2018.10.138>, 2019.

459 Lyell Sir, C., and Deshayes, G. P.: Principles of geology; being an attempt to explain the former changes of the earth's
460 surface, by reference to causes now in operation, J. Murray, London, 1830.

461 Magilligan, F. J., and Nislow, K. H.: Changes in hydrologic regime by dams, *Geomorphology*, 71, 61-78,
462 <https://doi.org/10.1016/j.geomorph.2004.08.017>, 2005.

463 Merritts, D., and Vincent, K. R.: Geomorphic response of coastal streams to low, intermediate, and high rates of uplift,
464 Medocino triple junction region, northern California, *GSA Bulletin*, 101, 1373-1388, [https://doi.org/10.1130/0016-7606\(1989\)101<1373:GROCST>2.3.CO;2](https://doi.org/10.1130/0016-7606(1989)101<1373:GROCST>2.3.CO;2), 1989.

466 Miodrag, S., and M, H. F.: 2-D Bed Evolution in Natural Watercourses—New Simulation Approach, *Journal of Waterway, Port, Coastal, and Ocean Engineering*, 116, 425-443, [https://doi.org/10.1061/\(ASCE\)0733-950X\(1990\)116:4\(425\)](https://doi.org/10.1061/(ASCE)0733-950X(1990)116:4(425)), 1990.

468 Nelson, N. C., Erwin, S. O., and Schmidt, J. C.: Spatial and temporal patterns in channel change on the Snake River
469 downstream from Jackson Lake dam, Wyoming, *Geomorphology*, 200, 132-142,
470 <https://doi.org/10.1016/j.geomorph.2013.03.019>, 2013.

471 Olsen, N. R. B.: Two-dimensional numerical modelling of flushing processes in water reservoirs, *Journal of Hydraulic Research*, 37, 3-16, <https://doi.org/10.1080/00221689909498529>, 1999.

473 Ota, Y., Chen, Y.-G., and Chen, W.-S.: Review of paleoseismological and active fault studies in Taiwan in the light of the
474 Chichi earthquake of September 21, 1999, *Tectonophysics*, 408, 63-77, <https://doi.org/10.1016/j.tecto.2005.05.040>, 2005.

475 Parker, G., and Izumi, N.: Purely erosional cyclic and solitary steps created by flow over a cohesive bed, *Journal of Fluid Mechanics*, 419, 203-238, <https://doi.org/10.1017/S0022112000001403>, 2000.

477 Petts, G. E., and Gurnell, A. M.: Dams and geomorphology: research progress and future directions, *Geomorphology*, 71,
478 27-47, <https://doi.org/10.1016/j.geomorph.2004.02.015>, 2005.

479 Seidl, M. A., and Dietrich, W. E.: The problem of channel erosion into bedrock, *Functional geomorphology*, 101-124, 1992.

480 Shafroth, P. B., Perry, L. G., Rose, C. A., and Braatne, J. H.: Effects of dams and geomorphic context on riparian forests of
481 the Elwha River, Washington, *Ecosphere*, 7, e01621-e01621, <https://doi.org/10.1002/ecs2.1621>, 2016.

482 Słowik, M., Dezső, J., Marciniak, A., Tóth, G., and Kovács, J.: Evolution of river planforms downstream of dams: Effect of
483 dam construction or earlier human-induced changes?, *Earth Surface Processes and Landforms*, 43, 2045-2063,
484 <https://doi.org/10.1002/esp.4371>, 2018.

485 Surian, N., and Rinaldi, M.: Morphological response to river engineering and management in alluvial channels in Italy,
486 *Geomorphology*, 50, 307-326, [https://doi.org/10.1016/S0169-555X\(02\)00219-2](https://doi.org/10.1016/S0169-555X(02)00219-2), 2003.

487 Tomkin, J. H., Brandon, M. T., Pazzaglia, F. J., Barbour, J. R., and Willett, S. D.: Quantitative testing of bedrock incision
488 models for the Clearwater River, NW Washington State, *Journal of Geophysical Research: Solid Earth*, 108,
489 <https://doi.org/10.1029/2001jb000862>, 2003.

490 Whipple, K. X., and Tucker, G. E.: Dynamics of the stream-power river incision model: Implications for height limits of
491 mountain ranges, landscape response timescales, and research needs, *Journal of Geophysical Research: Solid Earth*, 104,
492 17661-17674, <https://doi.org/10.1029/1999jb900120>, 1999.

493 Whipple, K. X.: Fluvial landscape response time: how plausible is steady-state denudation?, *American Journal of Science*,
494 301, 313-325, <https://doi.org/10.2475/ajs.301.4-5.313>, 2001.

495 Whipple, K. X., and Tucker, G. E.: Implications of sediment-flux-dependent river incision models for landscape evolution,
496 *Journal of Geophysical Research: Solid Earth*, 107, ETG 3-1-ETG 3-20, doi.org/10.1029/2000JB000044, 2002.

497 Whipple, K. X.: BEDROCK RIVERS AND THE GEOMORPHOLOGY OF ACTIVE OROGENS, *Annual Review of Earth and Planetary Sciences*, 32, 151-185, <https://doi.org/10.1146/annurev.earth.32.101802.120356>, 2004.

499 Williams, G. P., and Wolman, M. G.: Downstream effects of dams on alluvial rivers 1286, 1984.

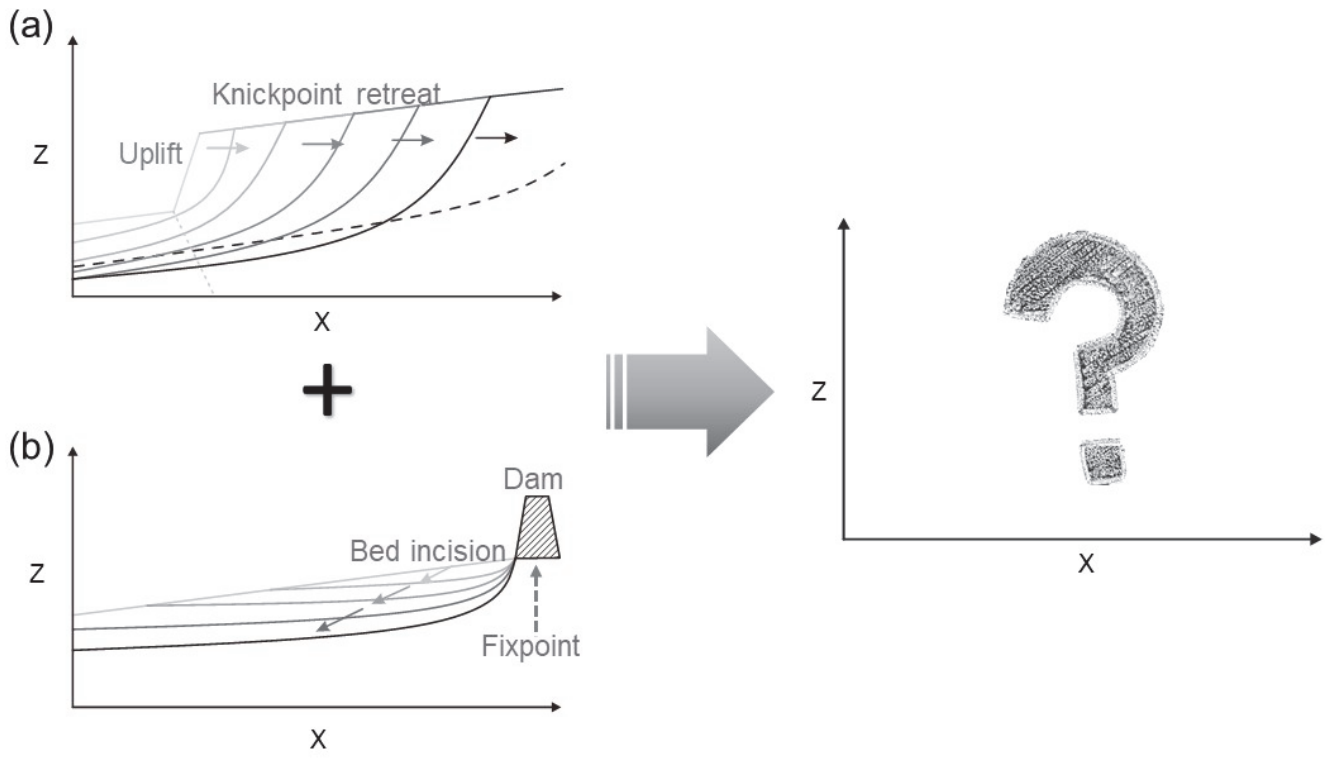
500 Zhou, M., Xia, J., Deng, S., Lu, J., and Lin, F.: Channel adjustments in a gravel-sand bed reach owing to upstream damming,
501 *Global and Planetary Change*, 170, 213-220, <https://doi.org/10.1016/j.gloplacha.2018.08.014>, 2018.

502

503

Table 1 Characteristics of the studied reaches of the Daan, Zhuoshui, and Dajia rivers

River	Time interval	Section	Bed Change		Channel Widening		Knickpoint retreat		C (m yr ⁻¹)	
			(m)	(m yr ⁻¹)	(m)	(m yr ⁻¹)	(m)	(m yr ⁻¹)		
Daan	2000–2004	a	-0.60	-0.15	-103.77	-25.94	85	21.25	22	
		b	-1.76	-0.44	47.50	11.88				
	2004–2007	a	-16.67	-5.56	-316.50	-105.50	422	140.67		
		b	-6.20	-2.07	-269.82	-89.94				
	2007–2011	a	2.06	0.52	19.30	4.83	412	103.00		
		b	-7.11	-1.78	-64.19	-16.05				
	2011–2016	a	-0.45	-0.09	31.19	6.24	--	--		
		b	-0.84	-0.17	41.27	8.25	--	--		
	Zhuoshui	1998–2008	c	-0.46	-0.05	-96.22	-9.62	--		--
			d	-2.24	-0.22	-130.41	-13.04			
e			-11.59	-1.16	-246.32	-24.63				
2008–2012		c	-5.44	-1.36	-258.44	-64.61	--	--		
		d	-2.77	-0.69	18.43	4.61				
		e	3.00	0.75	5.22	1.31				
2012–2015		c	-4.46	-1.49	-171.56	-57.19	--	--		
		d	-6.65	-2.22	-133.24	-44.41				
		e	-4.94	-1.65	-73.11	-24.37				
2015–2018		c	-0.84	-0.28	13.57	4.52	--	--		
		d	-0.86	-0.29	1.31	0.44				
		e	-3.03	-1.01	8.70	2.90				
Dajia		2000–2005	f	-2.39	-0.48	-14.12	-2.82	40	8.00	
			g	-2.02	-0.40	-116.44	-23.29			
		2005–2008	f	-2.57	-0.86	-39.90	-13.30	186	62.00	
	g		-7.50	-2.50	-142.97	-47.66				
	2008–2014	f	-1.33	-0.22	12.28	2.05	219	24.33		
		g	-0.38	-0.06	2.21	0.37				
	2010–2014	h	-4.20	-1.05	-25.45	-6.36				
	2014–2017	f	-1.39	-0.46	-10.44	-3.48				
		g	-3.32	-1.11	8.84	2.95				
		h	-5.27	-1.76	-20.63	-6.88				



506

507 Figure 1: Schematic diagrams of longitudinal profile development for (a) fault scarp's knickpoint, (b) dam's fixpoint,

508 and (c) How will the combined effects develop longitudinal profile?

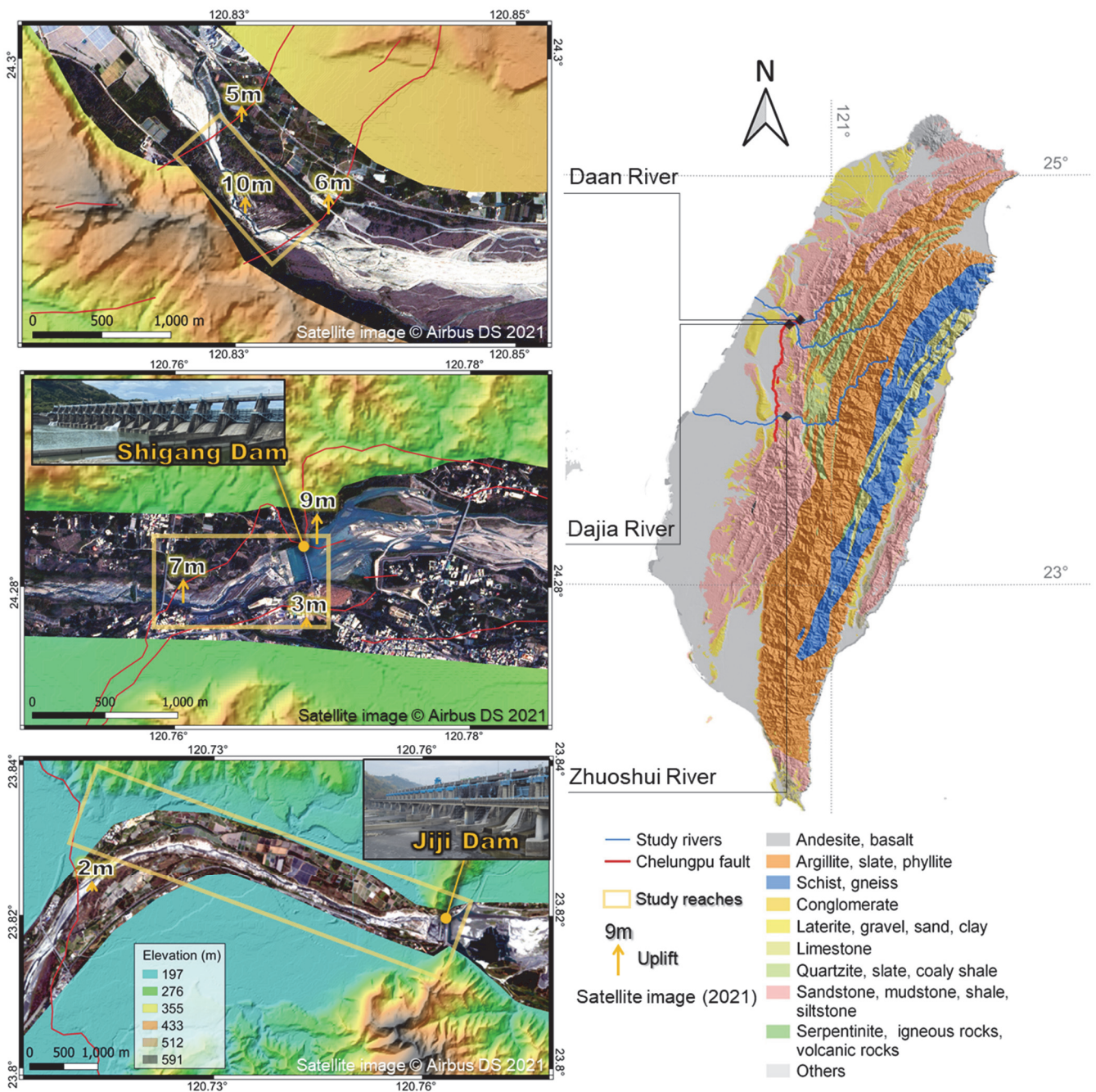
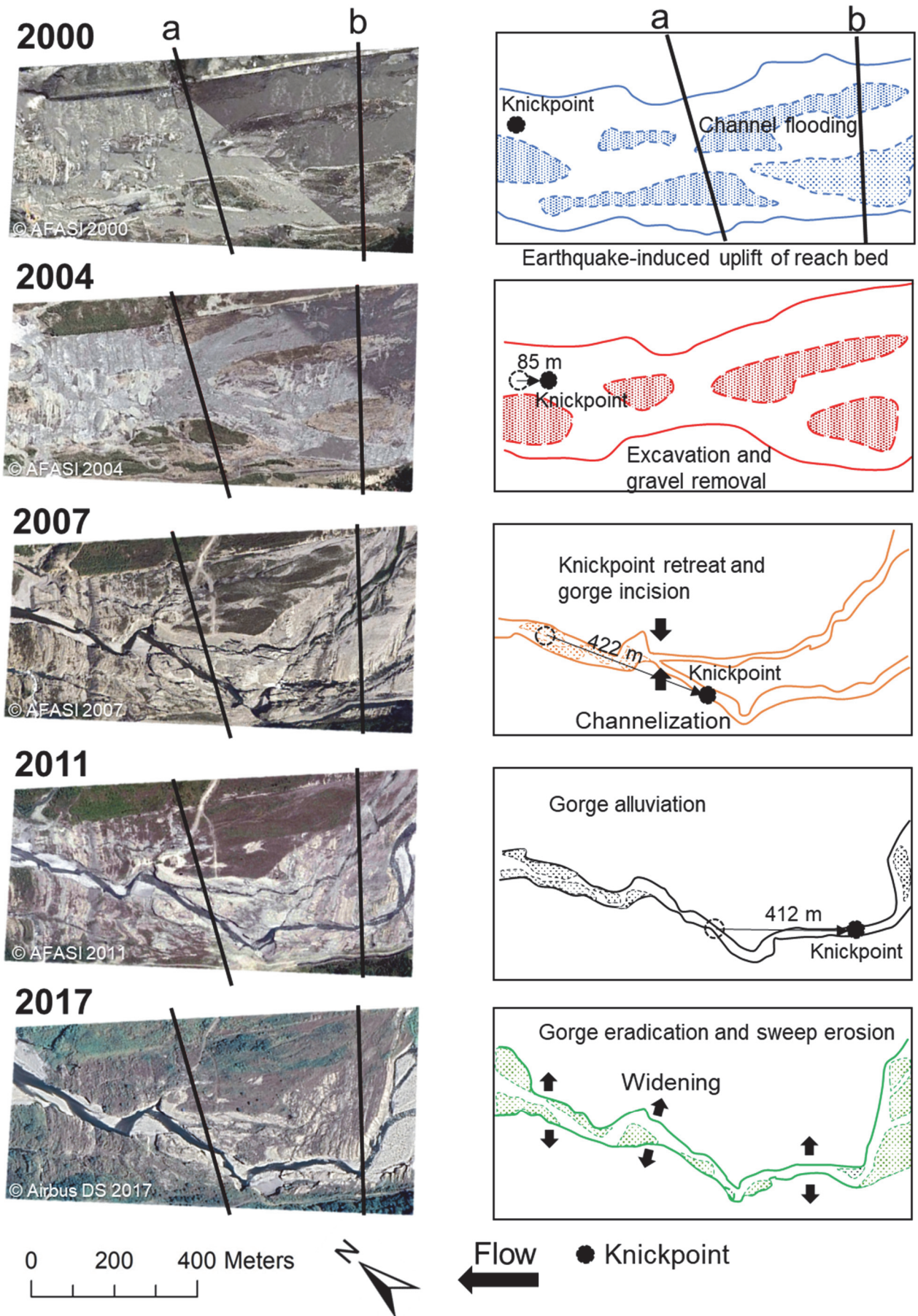
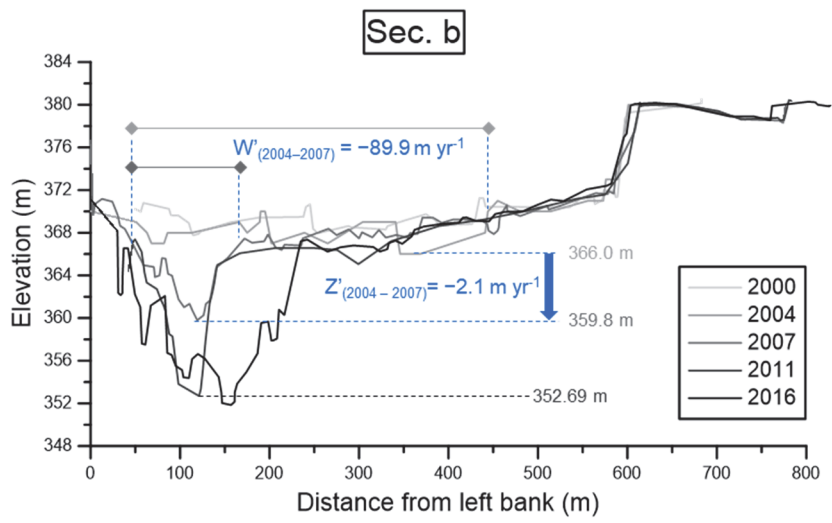
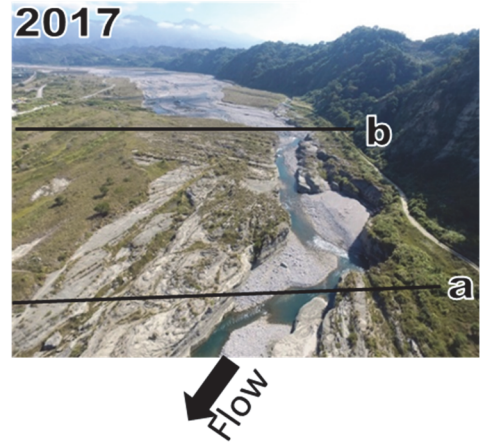
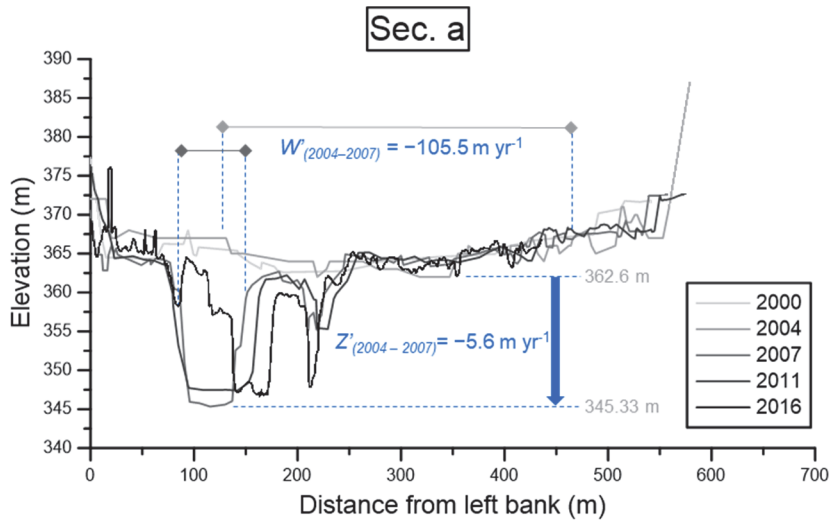


Figure 2: Locations of the Chelungpu Fault, the three studied rivers, and satellite images (from CSRSR/NCU [date: 05-Feb-2021, 2m resolutions](#)) showing the studied reaches.



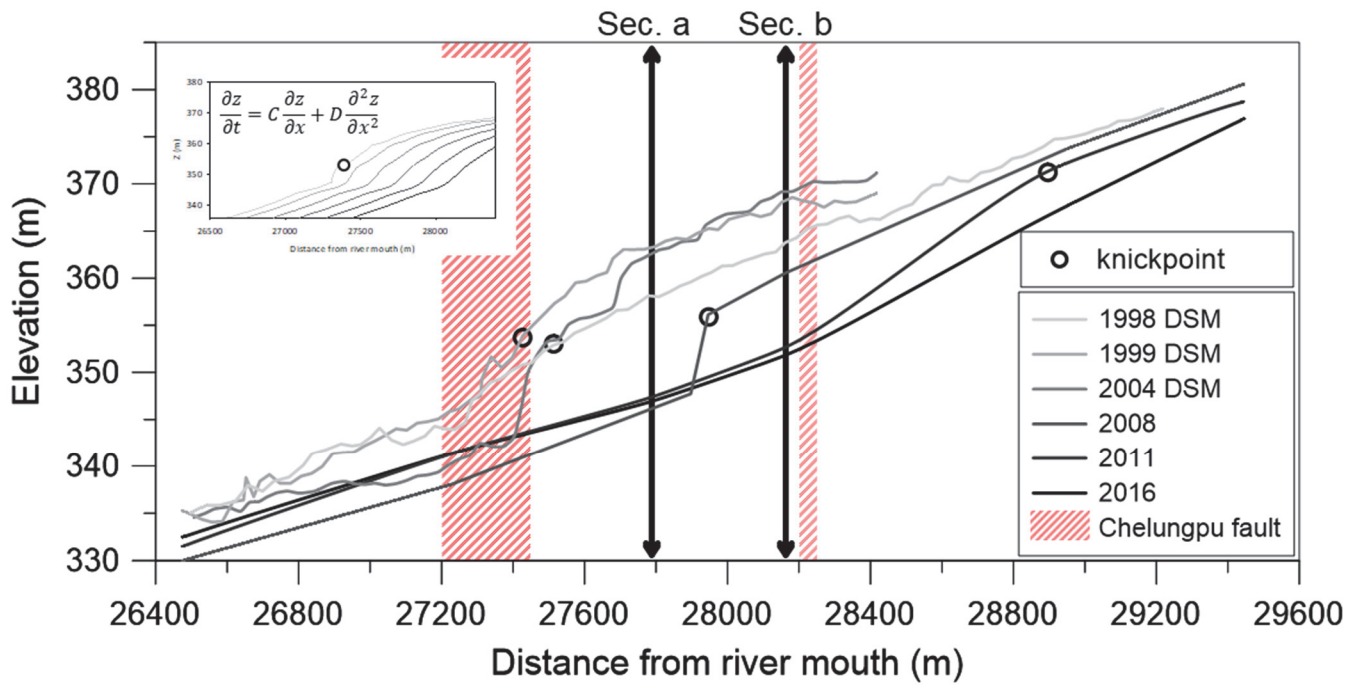
512
 513 **Figure 3: Orthographic images (2000–2011), satellite image (2017) and flow paths of the studied reach of the Daan**
 514 **River from 2000 to 2017.**



515

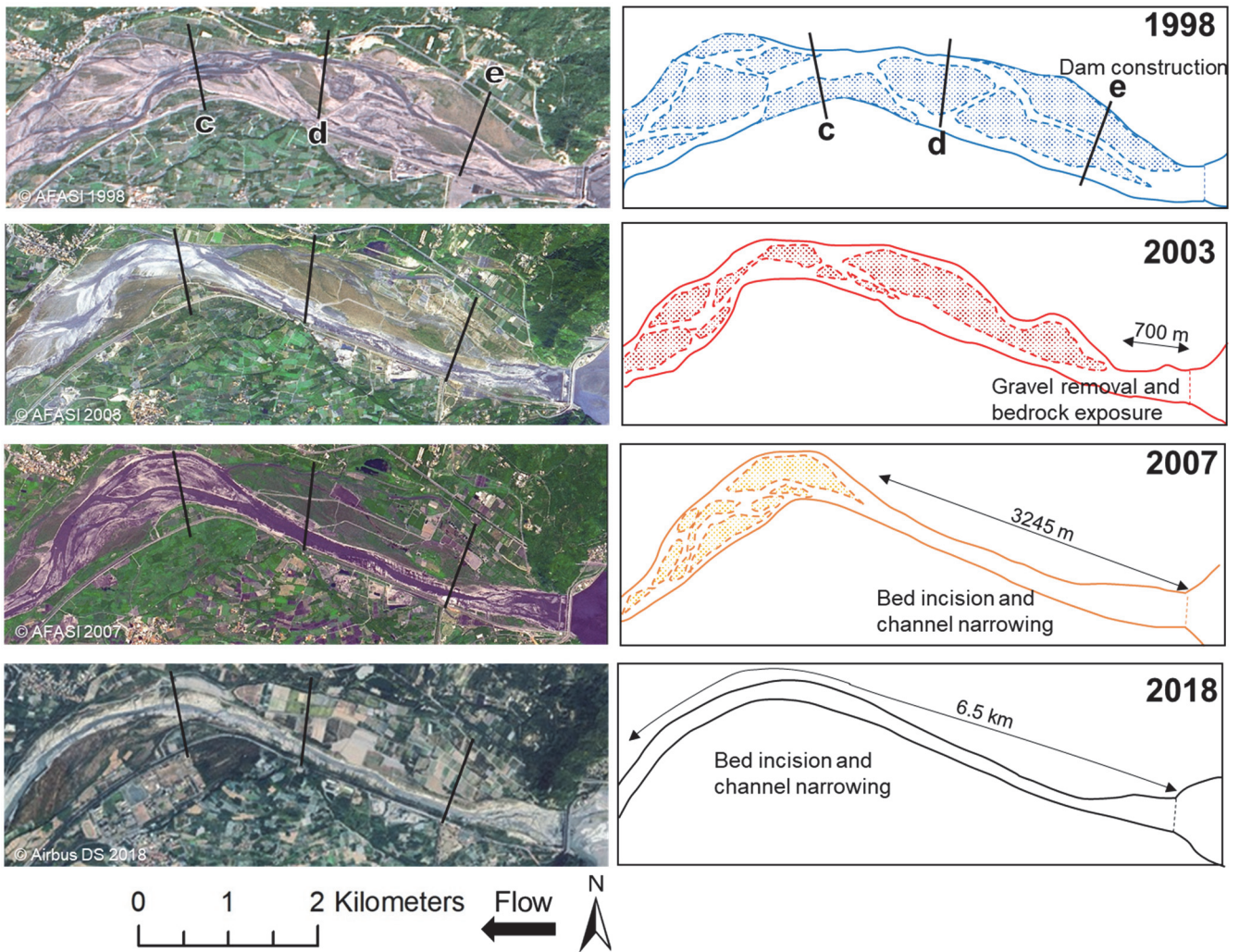
516 **Figure 4: Cross-sections a and b of the Daan River from 2000 to 2016 (from WRA).**

517



519

520 Figure 5: Longitudinal profiles of the studied reach of the Daan River from 2000 to 2016. Profiles for 1998–2008 are
 521 from Cook et al. (2013), and 2011–2016 are from WRA. Data between 1998 and 2004 are derived from aerial photograph
 522 generated Digital Surface Models (DSMs). Knickpoint retreats are simulated using the advective-diffusive model at the
 523 top left.
 524



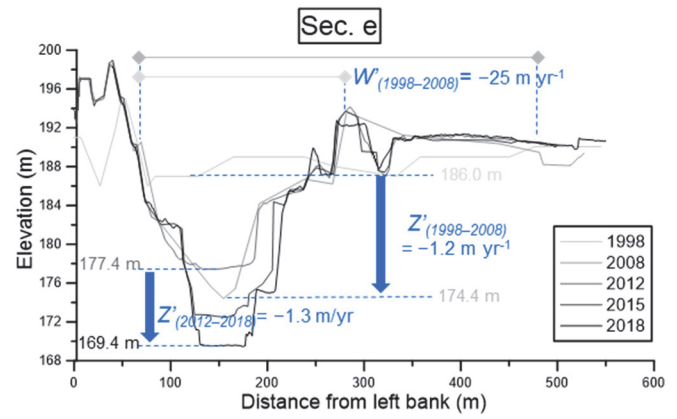
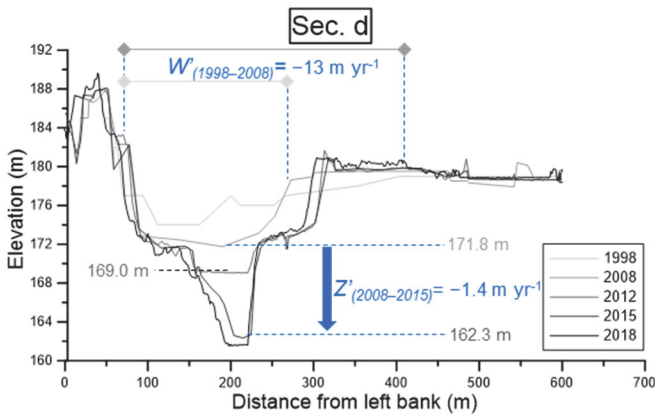
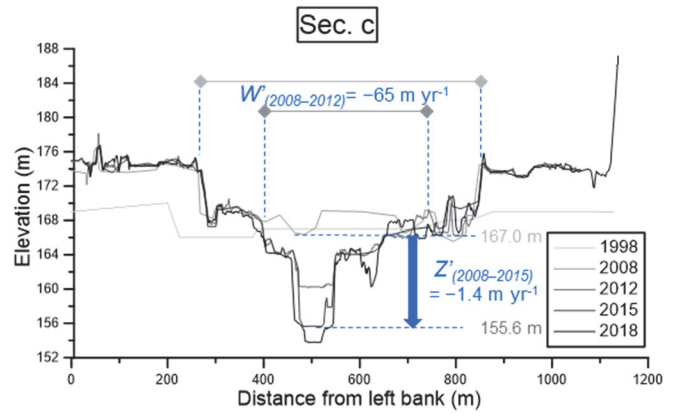
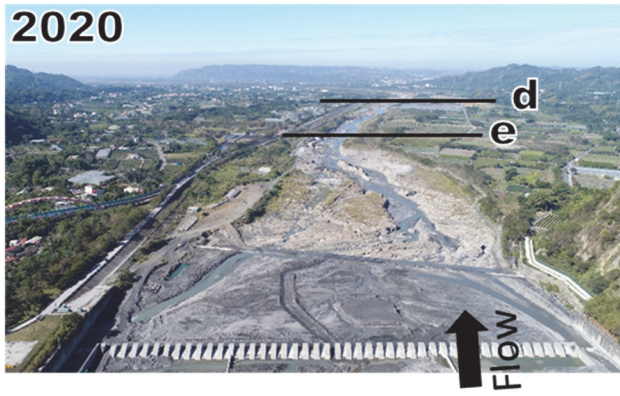
525

526

527

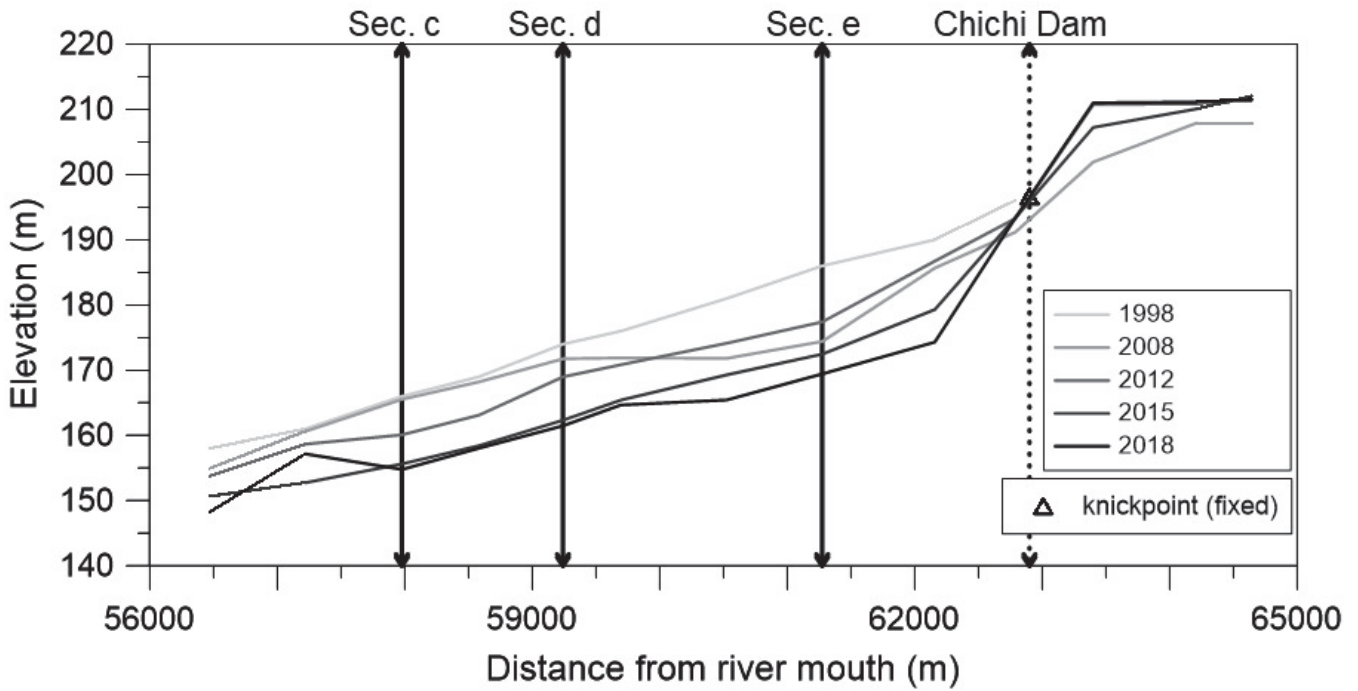
528

Figure 6: Orthographic images (1998–2007), satellite image (2018), and flow paths of the studied reach of the Zhuoshui River from 1998 to 2018.



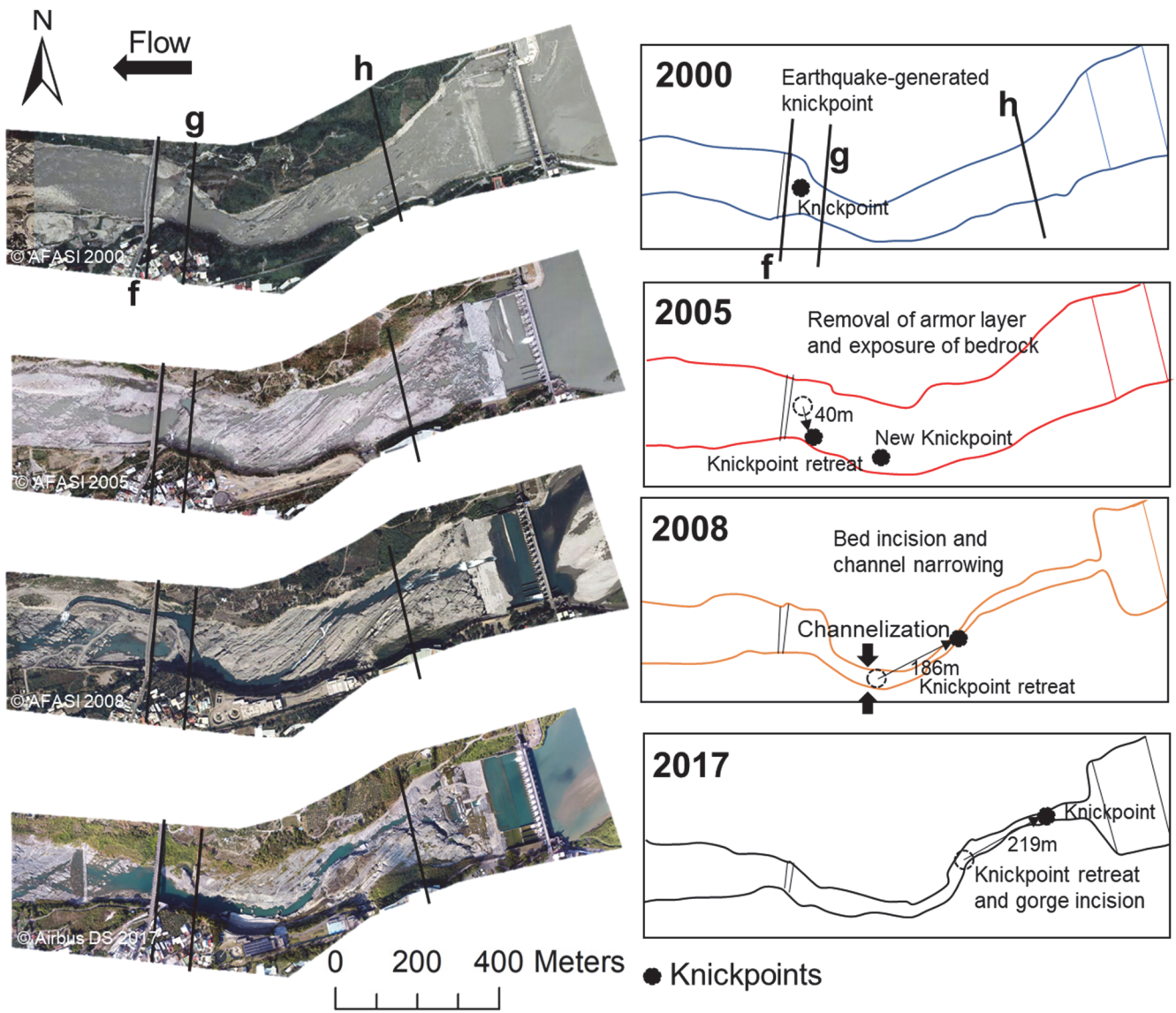
529
530

Figure 7: Profiles of cross-sections c, d, and e of the Zhuoshui River from 1998 to 2018 (from WRA).



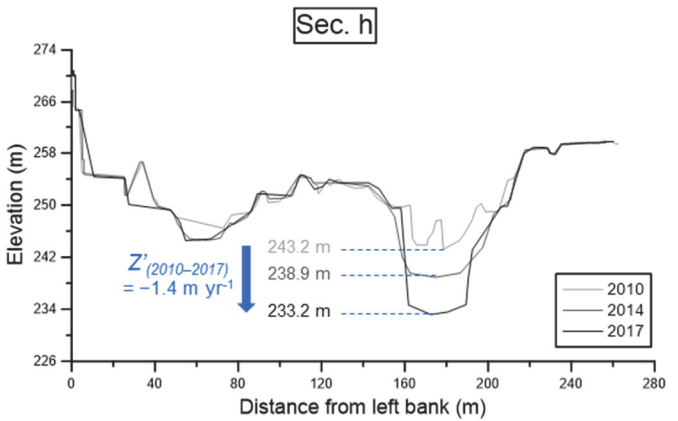
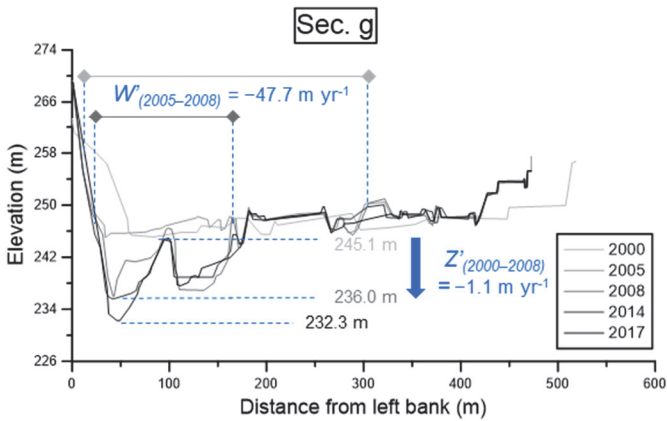
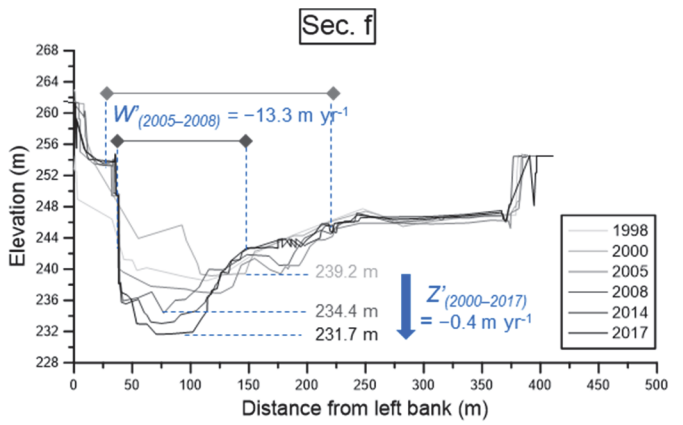
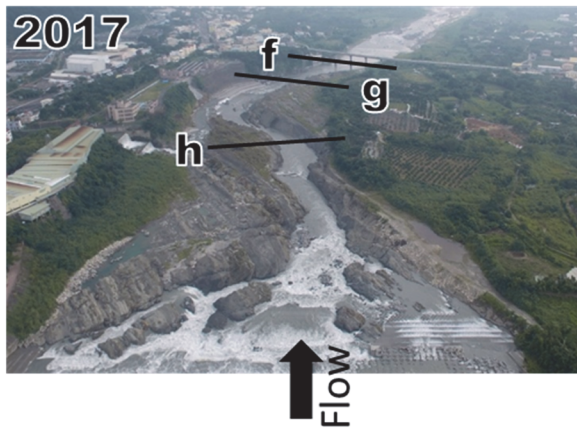
531
532

Figure 8: Longitudinal profiles of the studied reach of the Zhuoshui River from 1998 to 2018 (from WRA).



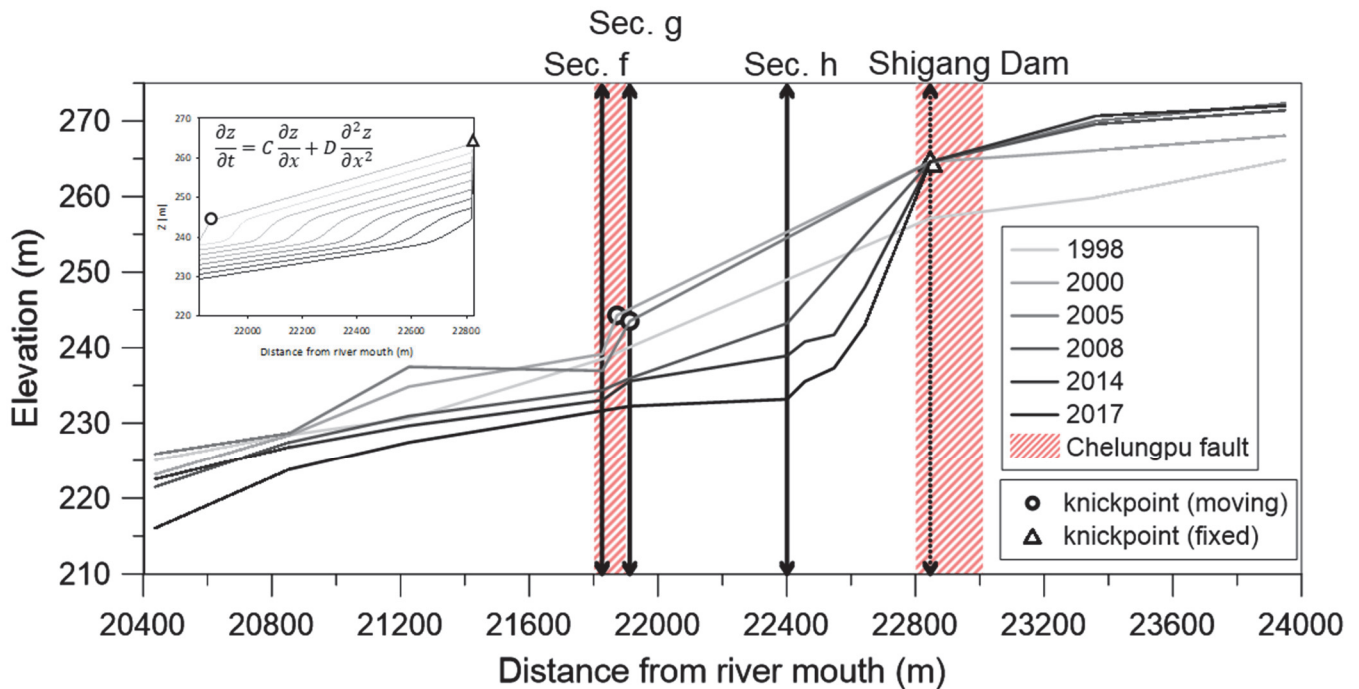
533
534
535

Figure 9: Orthographic images (2000–2008), satellite image (2017), and flow paths of the studied reach of the Dajia River from 2000 to 2017.



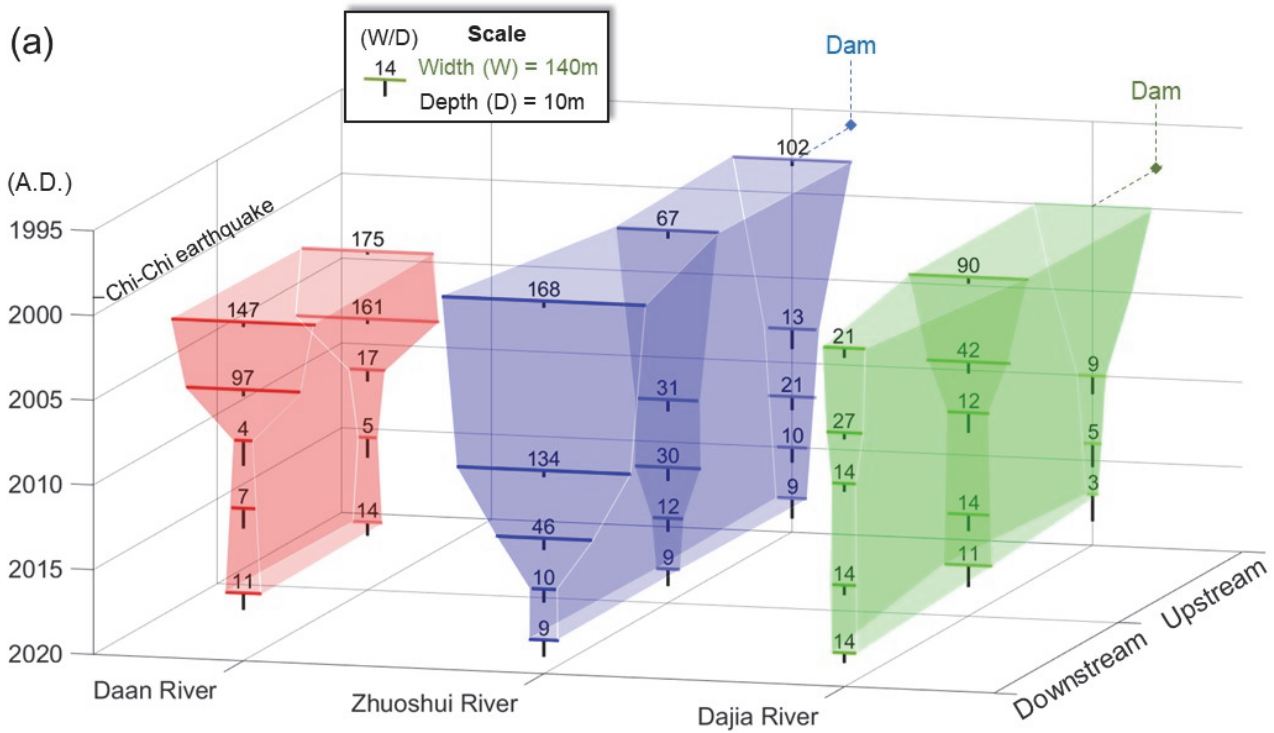
536
537

Figure 10: Cross-sections f, g, and h of the Dajia River from 2000 to 2017 (from WRA).

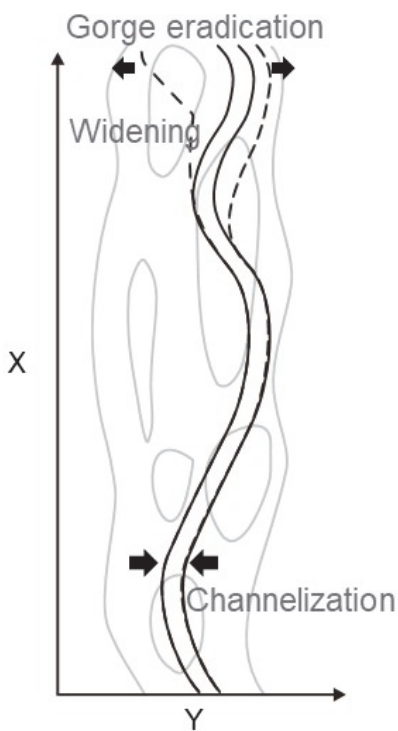


538
539
540
541
542

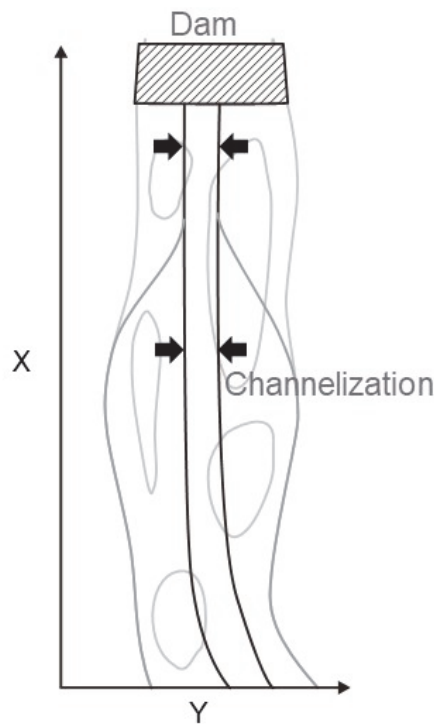
Figure 11: Longitudinal profiles of the studied reach of the Dajia River from 1998 to 2017 (from WRA). Knickpoint retreats are simulated using the advective-diffusive model at the top left.



(b) Daan river



(c) Zhuoshui river



(d) Dajia river

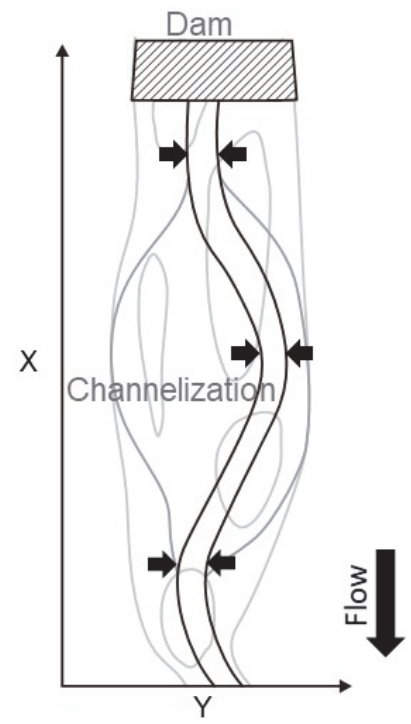
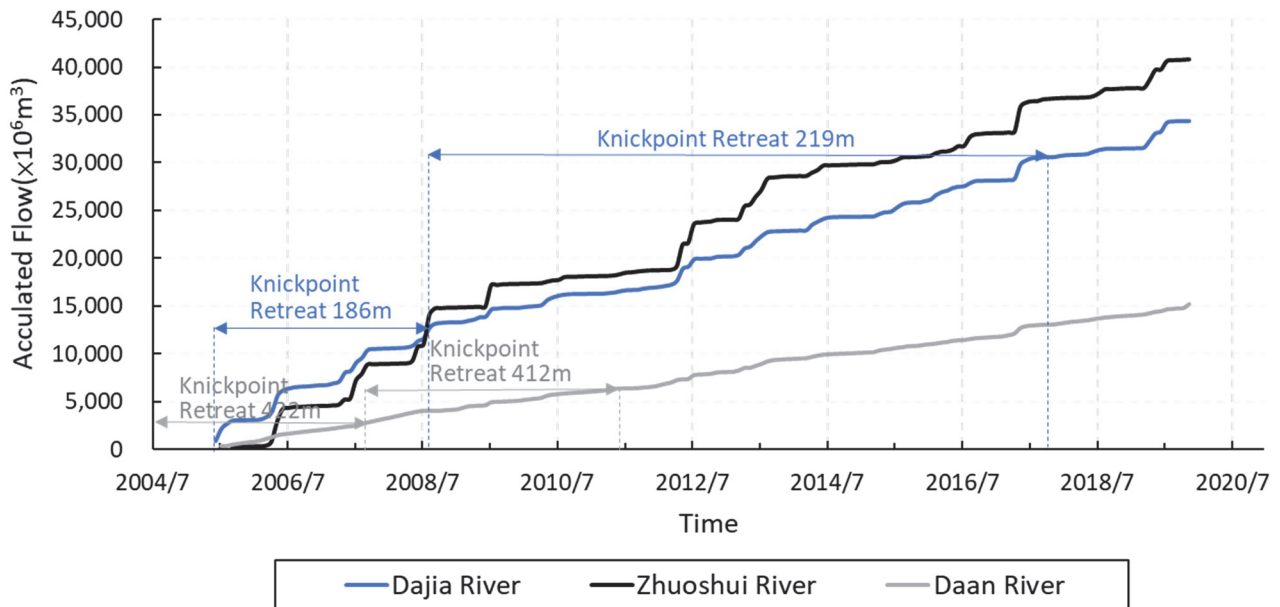
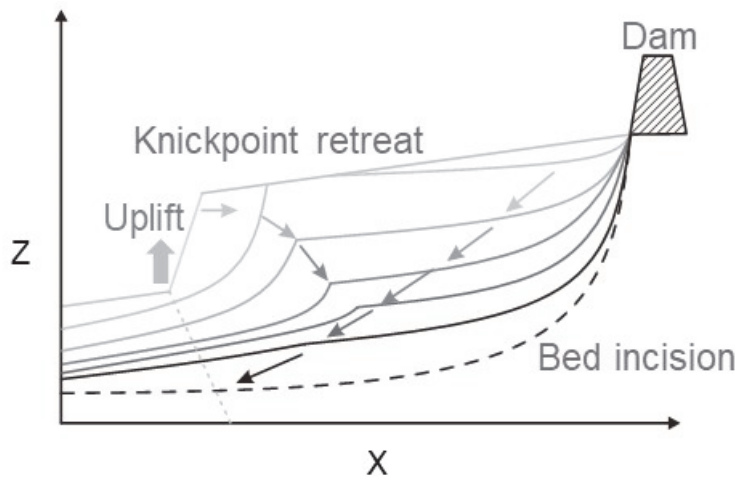


Figure 1212: (a) Channel width (W), depth (D), and aspect ratio (W/D) of the studied reaches of the three rivers. The aspect ratio was defined as the ratio of the bankfull width to the depth of the bankfull channel. The vertical axis shows the time from 1995 downward to 2020, the horizontal axis shows the rivers, and the normal axis shows the sections from downstream to upstream. Schematic diagrams of knickpoint retreat and river pattern development for (b) coseismic uplift, (c) dam obstruction, and (d) dam obstruction and coseismic uplift.



550
551

Figure 13: The cumulative flow in the three study reaches and the corresponding knickpoint retreat distances.



552
553
554
555
556

Figure 14: A Schematic diagram of longitudinal profile development for the combined effects from dam construction and coseismic uplift.